

# 1 Structural variant selection for high-altitude adaptation using single-molecule 2 long-read sequencing

3 Jinlong Shi<sup>1,2,4\*</sup>, Zhilong Jia<sup>1,2,3\*</sup>, Xiaojing Zhao<sup>2\*</sup>, Jinxiu Sun<sup>4\*</sup>, Fan Liang<sup>5\*</sup>, Minsung Park<sup>5\*</sup>, Chenghui Zhao<sup>1</sup>,  
4 Xiaoreng Wang<sup>2</sup>, Qi Chen<sup>4</sup>, Xinyu Song<sup>2,3</sup>, Kang Yu<sup>1</sup>, Qian Jia<sup>2</sup>, Depeng Wang<sup>5</sup>, Yuhui Xiao<sup>5</sup>, Yinzhe Liu<sup>5</sup>, Shijing  
5 Wu<sup>1</sup>, Qin Zhong<sup>2</sup>, Jue Wu<sup>2</sup>, Sajia Cui<sup>2</sup>, Xiaochen Bo<sup>6</sup>, Zhenzhou Wu<sup>7</sup>, Manolis Kellis<sup>8,9</sup>, Kunlun He<sup>1,2#</sup>

6 1. Key Laboratory of Biomedical Engineering and Translational Medicine, Ministry of Industry and Information  
7 Technology, Chinese PLA General Hospital, Beijing, China.

8 2. Beijing Key Laboratory for Precision Medicine of Chronic Heart Failure, Chinese PLA General Hospital, Beijing,  
9 China.

10 3. Research Center of Medical Artificial Intelligence, Chinese PLA General Hospital, Beijing, China.

11 4. Research Center of Medical Big Data, Chinese PLA General Hospital, Beijing, China.

12 5. GrandOmics Biosciences Inc, Beijing, China.

13 6. Beijing Institute of Radiation Medicine, Beijing, China.

14 7. BioMind Inc, Beijing, China.

15 8. Computer Science and Artificial Intelligence Laboratory, Massachusetts Institute of Technology, Cambridge,  
16 MA, USA.

17 9. Broad Institute of MIT and Harvard, Cambridge, MA, USA.

18 \*These authors contributed equally to this work.

19 #Corresponding author: [kunlunhe@plagh.org](mailto:kunlunhe@plagh.org)

20

## 21 Abstract: (150 words)

22 Structural variants (SVs) can be important drivers of human adaptation with strong effects, but previous studies  
23 have focused primarily on common variants with weak effects. Here, we used large-scale single-molecule long-  
24 read sequencing of 320 Tibetan and Han samples, to show that SVs are key drivers of selection under high-  
25 altitude adaptation. We expand the landscape of global SVs, apply robust models of selection and population  
26 differentiation combining SVs, SNPs and InDels, and use epigenomic analyses to predict driver enhancers,  
27 target genes, upstream regulators, and biological functions, which we validate using enhancer reporter and DNA  
28 pull-down assays. We reveal diverse Tibetan-specific SVs affecting the cis- and trans-regulatory circuitry of  
29 diverse biological functions, including hypoxia response, energy metabolism, lung function, etc. Our study greatly  
30 expands the global SV landscape, reveals the central role of gene-regulatory circuitry rewiring in human  
31 adaptation, and illustrates the diverse functional roles that SVs can play in human biology.

## 32 Introduction

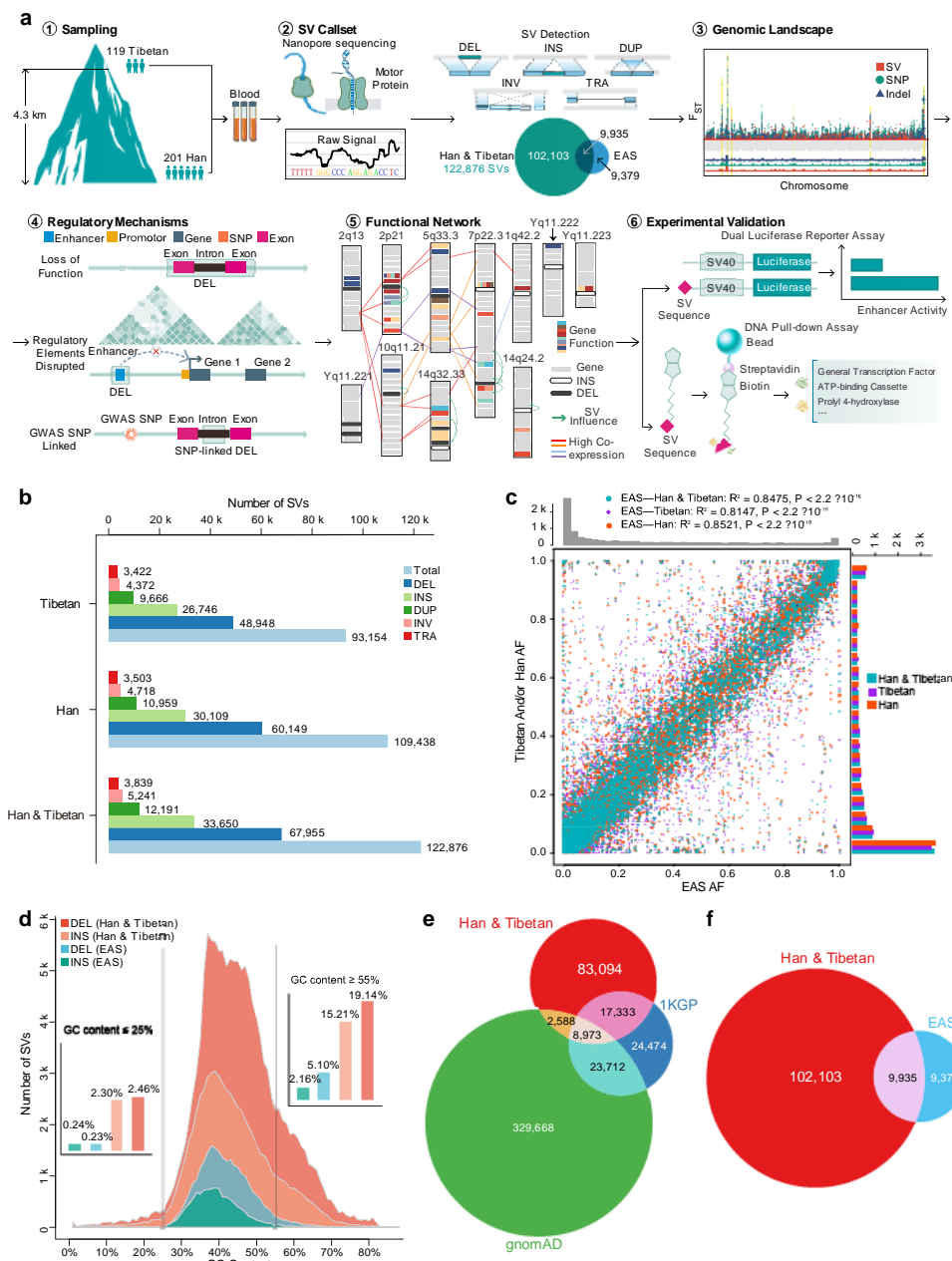
33 Structural variants (SVs) account for the majority of variable base pairs in the human genome and can cause  
34 dramatic alterations in gene function and gene regulation. They have been shown to play important biological  
35 roles in human biology and human disease<sup>1</sup>. For example, an inversion disconnecting TFAP2A from its  
36 enhancers causes branchiooculofacial syndrome<sup>2</sup>, and copy number differences in the AMY1 gene are

37 associated with high-starch diets or low-starch diets in the population<sup>3</sup>. Despite such dramatic examples, the  
38 roles of SVs in disease and in human evolutionary adaptation remain poorly studied, with most studies focusing  
39 instead on common single-nucleotide variants of weak effect, due in great part to technological limitations.

40 The adaptation of Tibetan people to high altitude provides an ideal model for studying adaptation during the  
41 evolutionary history of modern humans given its well-controlled context<sup>4-7</sup>, but this adaptation remains  
42 insufficiently studied at the population scale. Altitude sickness mainly takes the form of acute mountain sickness,  
43 high-altitude pulmonary oedema, and high-altitude cerebral oedema, which involve dizziness, headache, muscle  
44 aches, etc. The prevalence rate of these types of altitude sickness in the Tibetan population is lower than that in  
45 the Han population. Previous studies<sup>4,8</sup> have focused mainly on hypoxia-inducible factor (HIF) pathways,  
46 including those involving *EGLN1* and *EPAS1*, the latter of which shows a Denisovan-like haplotype in Tibetans<sup>6</sup>.  
47 However, these early studies relied on small sample sizes that were unlikely to reveal population genetic  
48 characteristics, used short-read next-generation sequencing (NGS) techniques that are not well suited for SV  
49 analysis, and lacked the sizable control cohorts of Han populations<sup>9</sup> necessary for revealing the unique genetic  
50 characteristics of Tibetan adaptation.

51 By contrast, long-read technologies, including single-molecule real-time (SMRT) and Oxford Nanopore  
52 Technologies (ONT) platforms, can provide a complete view of genomic variation. SVs can be important drivers  
53 of genome biological function and human evolutionary adaptation by enabling the rewiring of the long-range  
54 gene regulatory circuitry, amplification of gene clusters, and strong-effect adaptive changes that can involve  
55 multiple genes. Even in very small sample sizes, long-read sequencing has revealed extensive variation in SVs  
56 in the human population<sup>10</sup> and revealed that transposable elements, including long interspersed nuclear  
57 elements (LINEs) and short interspersed nuclear elements (SINEs) can be used to recapitulate the patterns of  
58 human evolution<sup>11</sup>, underlie most reported SVs<sup>10</sup>, and contribute to both medically important and evolutionarily  
59 selected variation<sup>12</sup>. However, the pattern of SV hotspots in the human genome remains incompletely understood,  
60 and comprehensive studies of large cohorts are needed to understand the role of SVs in human adaptation.

61 Here, we used long-read sequencing technologies to evaluate the roles of SVs in recent human adaptation (**Fig. 1a**). Our study reveals the first (unique) SV landscape for ethnic Han and Tibetan populations at a large scale.  
62 This work provides a large call set of 122,876 total SVs and contributes 102,103 novel SVs to the existing SV  
63 call set for East Asians. Unique patterns of SVs are also explored, which provides a different perspective for  
64 understanding genome evolution. Further comparisons of population stratification elucidate the comprehensive  
65 genetic landscape of the Han and Tibetan populations, revealing the potential roles of SVs in evolutionary  
66 adaptation to the high altitudes inhabited by Tibetans. We provide high-altitude adaptation candidate SVs,  
67 showing their functional impacts on enhancers, exons and the 3D genome. We show the functional connections  
68 between SV-associated genes and the unique traits of Tibetans. These findings implicate multiple genes in  
69 biologically relevant pathways, including the HIF, insulin receptor signalling, inflammation, and glucose and lipid  
70 metabolism pathways. Moreover, experimental validation confirms our analytical result showing that the most  
71 Tibetan-specific SV, a deletion downstream of *EPAS1*, disrupts the super enhancer in this genomic area in  
72 Tibetans and affects the binding of regulatory molecules critical for gene transcription activities. Our study  
73 expands the known East Asian and global SV sets and highlights the functional impacts and adaptation of SVs  
74 in Tibetans via complex cis- and trans-regulatory circuitry rewiring.



76

**Figure 1. SV discovery in 119 Tibetan and 201 Han samples.** **a.** Summary of the experimental pipeline. Overall, 320 Han and Tibetan samples were collected and sequenced via the ONT platform, resulting in 122,876 SVs. Candidate SVs for high-altitude adaptation, their functional regulatory mechanisms based on their connections with exons, enhancers and TAD boundaries, and candidate genes for high-altitude adaptation were explored. Cis- and trans-regulatory circuitry rewiring was validated in two biological assays. **b.** The numbers of 5 types of SVs in Han, Tibetan, and all samples. The majority are deletions and insertions. **c.** Allele frequency consistency between the SVs in the Han and Tibetan cohort and the 1KGP EAS cohort. The high consistency between them indicates the high quality of our SV call set. **d.** GC content distribution of insertions and deletions in the Han and Tibetan cohort and the EAS cohort, indicating that the ONT platform performs well even in genomic regions with a biased GC content. **e.** Overlap between the SVs of our cohort and 1KGP and gnomAD cohorts, showing 83,094 novel SVs. **f.** Overlap between the SVs of our cohort and the 1KGP EAS cohort, showing a 6-fold increase in the number of previously annotated East Asian SVs.

89

## **Results:**

### **90 1. Constructing and validating the *de novo* SV call set**

#### **91 SV discovery and quality evaluation**

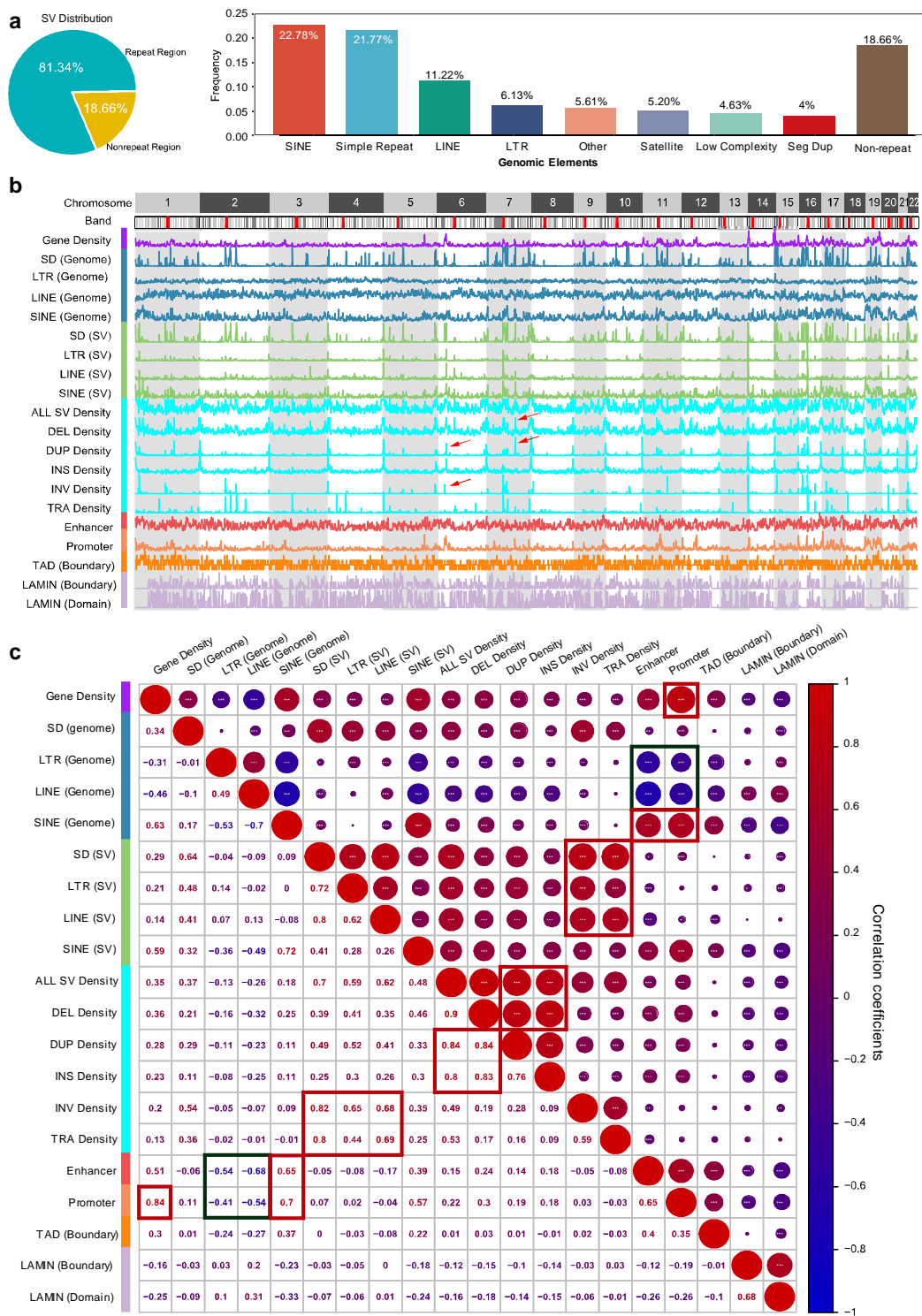
92 We sequenced the genomes of 201 Han and 119 Tibetan individuals using the ONT PromethION platform with  
93 an average depth of 21-fold coverage (**Supplementary Table 1a**). We detected 109,418 SVs in the Han  
94 population and 93,154 SVs in the Tibetan population (**Fig. 1b**), resulting in 122,876 SVs in total (89% and 76%,  
95 respectively). These SVs consisted of 67,955 deletions, 33,650 insertions, 12,191 duplications, 5,241 inversions,  
96 and 3,839 translocations. Each sample, averagely contains 20,741 SVs, including 8,520 insertions, 9,392  
97 deletions, 1,908 duplications, 548 inversions and 373 translocations (**Supplementary Fig. 1a** and  
98 **Supplementary Table 1a**). The numbers of different types of SVs showed no large difference in each Han and  
99 Tibetan sample (**Supplementary Fig. 1a**). Remarkably, in 50% of our samples, more than 90% of the SVs in  
100 the Han and Tibetan populations were captured, indicating that our sample size was sufficient to  
101 comprehensively profile the SV landscape of the Han and Tibetan populations (**Supplementary Fig. 1b-d**).

102 We used several lines of evidence to confirm the high quality of our Han and Tibetan SV call set. First, the  
103 manual curation of 298 SVs across all samples showed 94% accuracy (**Supplementary Table 1b**). Second, the  
104 PCR validation of 4 SVs in 57 samples showed 96% accuracy (**Supplementary Table 1c**). Third, our SV allele  
105 frequencies showed a Pearson correlation of 0.92 with the East Asian (EAS) database of the 1000 Genomes  
106 Project (1KGP) phase 3 (**Fig. 1c**). Fourth, 74% (13,342) of the SVs were shared between the sequencing results  
107 obtained for one sample using both the ONT (12.2X depth, 36.59 Gb, 18,002 SVs) and SMRT circular consensus  
108 sequencing (15.4X depth, 452 Gb, 20,617 SVs) platforms (**Supplementary Tables 1d, 2, 3**)<sup>13</sup>. Notably, 71%  
109 (12,429) of the SVs were shown to be shared when the new version of Guppy (3.0.5) was used (**Supplementary**  
110 **Table 3**), indicating no significant change in the overall quality of the SV call sets. These results collectively  
111 indicate the high quality of the SV call set. Accordingly, we provide an authoritative new reference set for future  
112 studies of genetic variation.

113 We also confirmed that the long-read sequencing platform performed well even in genomic regions with a GC-  
114 biased base composition. We compared the GC composition of deletions and insertions, two major types of SV,  
115 identified in our Han and Tibetan cohort and the EAS population of the 1000 Genomes database. The ONT  
116 platform revealed more SVs in total and more SVs in GC-biased areas than with NGS in the EAS population.  
117 For example, among all 67,954 deletions discovered using the ONT platform, 19.14% of the deletions were  
118 located in the high-GC content ( $\geq 55\%$ ) areas. Among all 12,969 deletions discovered using the NGS platform,  
119 only 5.10% of deletions were identified in high-GC content areas (**Fig. 1d**). This indicates the advantages of long-  
120 read sequencing for calling SVs, especially in genomic regions with a GC-biased base composition.

#### **121 Comparison with existing SV call sets**

122 We contribute a large number of new SVs and provide a useful reference panel for Chinese, East Asian, and  
123 worldwide populations. As an indicator of the near completeness of the SV results, we found that the majority of  
124 the identified SVs were shared between the Han and Tibetan populations and that the number of SVs in the Han  
125 population increased by only 17%, despite profiling almost twice as many Han as Tibetan genomes. We  
126 compared our SV set with two NGS-based SV call sets, those of the 1KGP<sup>14</sup> and the Genome Aggregation  
127 Database (gnomAD)<sup>15</sup>. Approximately 28,894 SVs included in the 1KGP and gnomAD sets were reidentified in  
128 our call set (**Fig. 1e**). Importantly, our study expands the total number of SVs in global SV databases by ~37%,  
129 by adding 83,094 novel SVs, and increases the number of EAS SVs to 121,417, by contributing 102,103 novel  
130 SVs (**Fig. 1f**). The application of ONT sequencing clearly contributed greatly to the increase in the number of  
131 SVs.



132  
133  
134  
135  
136  
137  
138

**Figure 2. SV composition, length frequency, and chromosome distributions.** **a.** SV proportions in different genome regions. The majority of SVs are associated within repeat elements, such as LINEs and SINEs as shown in the pie chart. **b.** Densities of repeats and their-associated SVs, all SVs, regulatory elements and genes in the genome. There are hotspots (peaks with red arrow) of SVs in the genome. **c.** Correlations between repeat elements, their-associated SVs, regulatory elements and genes in the genome. Different types of SVs are highly positively (red) inter-correlated. High correlation coefficients are boxed (red for positive and blue for negative).

139 Long-read sequencing of a large-scale sample of individuals is necessary for comprehensive population-scale  
140 SV profiling. We compared our SV set with an SV set derived from 15 samples using the SMRT platform<sup>10</sup>.  
141 Notably, 61,502 SVs (~61.7%) in our SV set were merged into 36,528 SVs (insertion length was ignored during  
142 SV merging due to the absence of this information for the 15 genomes). Nevertheless, 74,138 novel SVs  
143 (**Supplementary Fig. 1e**) were identified compared with the SV set based on the 15 genomes. Furthermore,  
144 59,878 novel SVs were found in our study (**Supplementary Fig. 1f**), the majority of which were low-frequency  
145 (allele frequency<0.1, ~58%) and singleton SVs (~29.9%) (**Supplementary Table 4**). We also compared our  
146 Tibetan SV set with the ZF1 SV call set, which was recently collected from a high-quality de novo assembled  
147 Tibetan genome based on the SMRT platform<sup>16</sup>. We found that only 15,890 SVs (~17%) in our Tibetan SV  
148 reference panel overlapped with the ZF1 SV call set (17,714 SVs) (**Supplementary Table 5**). A number of SVs  
149 overlapping with other publicly available SV sets verified the high quality of our Han and Tibetan SV set from  
150 another perspective. Thus, we provide a high-quality SV call set for a large-scale Han and Tibetan cohort.

151 2. *Genome-wide properties of SVs*

152 **The SV landscape in the Han-Tibetan population**

153 More SVs are distributed in repeat regions, such as regions containing transposable elements and satellite  
154 repeat regions. SVs showed 4-fold enrichment in repeat elements (81% occurred in repeats), including 40% of  
155 SVs in transposable elements (23% SINEs, 11% LINEs, 6% LTRs) and 27% in satellite repeat regions (22% in  
156 simple repeats, 5% satellite repeats) (**Fig. 2a**). SVs were 1.8-fold enriched in SINEs (23% vs. 13% expected)  
157 but 1.9-fold depleted in LINEs (11% vs. 22% expected) (**Fig. 2a**), possibly due to the increased selective pressure  
158 related to their longer length<sup>17</sup>. Within different allele frequency intervals, more SVs were distributed in repeat  
159 regions (**Supplementary Table 6**). These repeats are more likely to produce SVs because repeats are prone to  
160 non-allelic homologous recombination, replication slippage, and non-homologous end-joining<sup>18</sup>.

161 The different types of SVs are distributed among different types of repeat and functional elements in a biased  
162 manner. The enrichment among these elements differed among different SV types, with deletions, insertions,  
163 and duplications being associated with SINEs, LINEs, and simple repeats and inversions and translocations  
164 being associated with LINEs and satellite repeats (**Supplementary Table 7**). The SV length distribution showed  
165 two distinct peaks, at ~300 bp (Alu) and ~6 kb (LINE) (**Supplementary Fig. 2a, 2b**). Exonic SVs showed 6-fold  
166 enrichment relative to the exons in the genome (**Supplementary Fig. 2c, Supplementary Table 8**). LINE-  
167 associated SVs showed 2-fold depletion in intronic regions and a 5-fold enrichment in exonic regions  
168 (**Supplementary Fig. 2c, Supplementary Table 8**). Concerning the SINE- and LINE-mediated SVs, duplications  
169 and inversions were >5-fold enriched in exons, while deletions were 40% depleted and insertions were 30-fold  
170 depleted in exons (**Supplementary Fig. 2d, Supplementary Table 8**), suggesting deleterious effects of SINE-  
171 and LINE-mediated insertions on the genome overall. The majority of SVs (75% SVs) occur at a low frequency  
172 (7.8%), while a greater number of higher-frequency insertions are maintained relative to other types of SVs  
173 (**Supplementary Fig. 2e**).

174 **SV hotspots in the genome**

175 SV hotspots in the genome were indicated by the extremely high density of SVs in certain regions relative to  
176 other regions in the whole genome (**Fig. 2b**). For example, there were 58 C7orf50-associated SVs, indicating  
177 that this region is prone to DNA breaks and the formation of SVs (**Supplementary Fig. 2f**). Deletions, insertions,  
178 and duplications showed a highly inter-correlated distribution in the genome (**Supplementary Fig. 2c**). The  
179 distributions of LINE-associated SVs, SD-associated SVs and translocations were also highly inter-correlated,  
180 whereas the distributions of LINEs and SDs in the human genome were anti-correlated. These results revealed  
181 clear SV hotspots in the genome. As promoters and enhancers are correlated with SINEs, they are also  
182 correlated with SINE-associated SVs. Notably, the distributions of promoters and enhancers were correlated

183 with those of deletions, duplications, insertions, SINE-related SVs and SINEs but anti-correlated with those of  
184 LINEs and LTRs in the genome. This indicates that SINE-associated SVs, deletions, duplications, and insertions  
185 play more important roles in regulating gene transcription than other types of SVs.

#### 186 Preferential evolutionary selection for SVs

187 We also found that SVs were very infrequent in exonic regions (17%), upstream regions (0.5%), 3'-UTRs (0.34%),  
188 and 5'-UTRs (0.16%), where they are more likely to disrupt functional elements, but that they were very abundant  
189 in intronic regions (30%) and intergenic regions (46%), where they are less likely to be disruptive  
190 (**Supplementary Fig. 2c**). This difference was also observed in the fraction of fully penetrant (allele frequency=1  
191 within the corresponding population) SVs vs. singleton SVs in each population, with a larger fraction of exonic  
192 SVs being singletons and a larger fraction of intronic and intergenic SVs being shared, consistent with continued  
193 evolutionary pressures acting on SV allele frequency in each population (**Supplementary Fig. 2h** and  
194 **Supplementary Table 1e**).

195 Genome evolution selects and preserves more repeat-associated SVs. We found that in both the Han and  
196 Tibetan populations, fully penetrant SVs were ~6.6 times more frequent in repeat regions than in non-repeat  
197 regions, while singleton SVs (found in only one individual in a given population) were only ~3.8 times more  
198 frequent in repeat regions than in non-repeat regions (**Supplementary Fig. 2g**). This indicates that SVs are  
199 preferentially excluded (singletons) from non-repeat regions, where they are more likely to disrupt functional  
200 elements, and that they are preferentially tolerated (high allele frequency) in repeat elements, where they  
201 accumulate over evolutionary time.

202 We also found that while deletions and insertions were similarly abundant in the genome, deletions were more  
203 likely to be singletons than to be shared, while insertions were more likely to be shared than to be singletons  
204 (**Supplementary Fig. 2i, SupplementaryTable 1e**), indicating that deletions are more likely to disrupt elements  
205 than insertions.

206 In summary, our comparisons of the frequency of SVs in different genomic regions and of the relative frequencies  
207 of singletons and shared SVs indicate the preferential retention of repeat-associated SVs, intronic SVs and  
208 insertions vs. deletions, suggesting that these variant types are less likely to disrupt genomic functions.

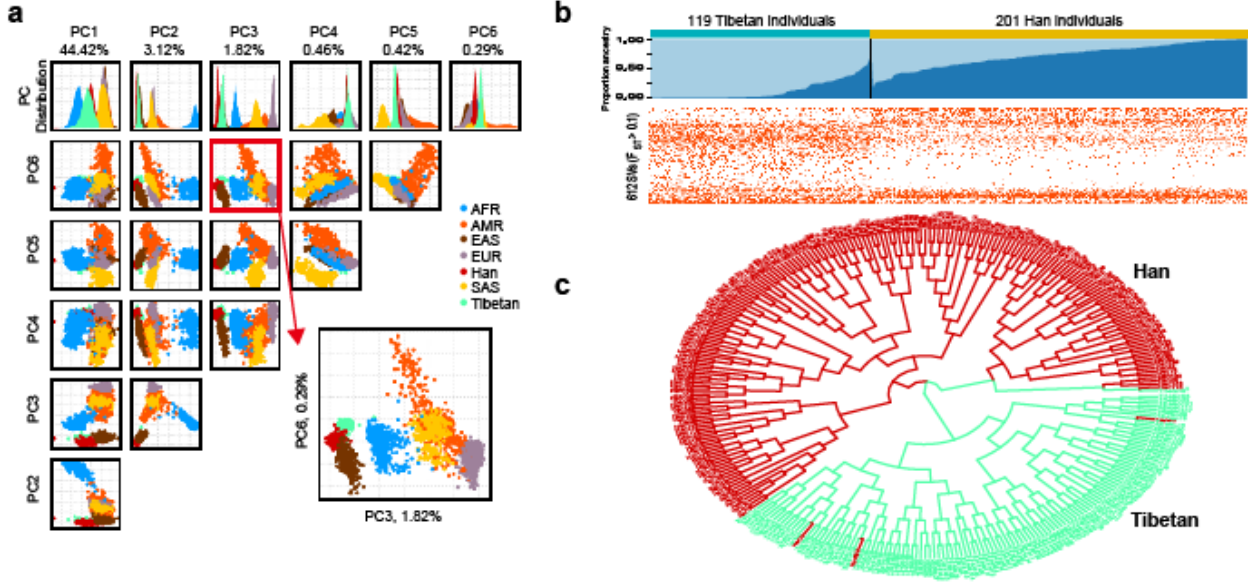
### 209 3. *Population genetics of Han-Tibetan populations and the role of functional SVs in evolutionary 210 adaptation*

#### 211 SVs are a representative ethnic characteristic

212 The Han and Tibetan SV call sets provide an unprecedented resource for the in-depth analysis of genomic  
213 variations for comparisons between Han and Tibetan populations. The Han and Tibetan cohorts shared 79,716  
214 SVs (**Supplementary Fig. 3a**). A principal component analysis (PCA) established that SVs could be used to  
215 clearly distinguish these two very closely related populations (**Supplementary Fig. 3b**). These results suggested  
216 the existence of significant genetic differences between the Han and Tibetan populations based on SVs alone,  
217 which are usually revealed by SNP analysis. When we extended the PCA to other populations from the 1KGP  
218 database, such as African, American, EAS, European, and South Asian populations, the Han and Tibetan  
219 populations were shown to be closely related to EAS populations and distant from these other populations (**Fig.**  
220 **3a**). This indicates that the Tibetan population is genetically closer to the Han population than to other populations  
221 and that these populations probably originated from a single common ancestor. Admixture analysis using the SV  
222 call set clearly showed separation between the Han and Tibetan populations (**Fig. 3b**, top). The hierarchical  
223 clustering of the SVs with  $F_{ST} > 0.25$  also showed that the Han and Tibetan populations possess ethnicity-specific  
224 SVs as well as common SVs (**Fig. 3b**, bottom). Evolutionary tree analysis based on all the SVs also showed a  
225 clear separation between Han and Tibetan with 3 sample exception (**Fig. 3c**). These results demonstrate that

226 SVs, in addition to SNPs, are a powerful proxy for distinguishing genetically closely related populations as a  
227 representative characteristic of an ethnic group.

228



229

230 **Figure 3. Population genetics of Han-Tibetan populations.** **a.** PCA of the SV call sets of the Tibetan and Han  
231 cohorts and 1KGP African (AFR), American (AMR), East Asian (EAS), European (EUR) and South Asian (SAS)  
232 cohorts. The Han (red) and Tibetan (green) populations are close to the EAS (brown) populations, as expected,  
233 and can be clearly separated according to PC3 and PC6. **b.** Population structure of the Tibetan and Han  
234 populations. Admixture analysis (top), clustered SVs with an  $F_{ST} > 0.1$  (bottom). The SVs can distinguish two  
235 populations, although the number of SVs per individual in the two populations is similar. **c.** A clear separation  
236 between Han and Tibetan with 3 sample exception in the evolutionary tree analysis based on all the SVs of Han  
237 and Tibetan (green).

238

### Genetic landscapes of Han-Tibetan populations

239 SVs, InDels, and SNPs function synergistically to allow Tibetans to live in high-altitude environments. We  
240 complemented our long-read sequencing results with deep short-read sequencing in 148 samples and carried  
241 out a comprehensive comparison of the Han-Tibetan genome based on population NGS/TGS sequencing data,  
242 comprehensively revealing the genomic signals of evolutionary selection for high-altitude adaptations. A  
243 Manhattan plot based on SNPs, InDels, and SVs between the Han and Tibetan populations revealed clear  
244 evolutionary selection (Fig. 4a). The selection for these 3 types of genetic variations was highly consistent in  
245 multiple genomic regions, and several regions were found to differ significantly between the Han and Tibetan  
246 populations (Supplementary Fig. 4a). For example, there are many SNPs, InDels, and SVs in the region around  
247 EGLN1 on chromosome 1 (Fig. 4b) and the region around EPAS1 on chromosome 2 (Fig. 4c), forming several  
248 plateaus of evolutionary selection in the Manhattan plot of the human genome.

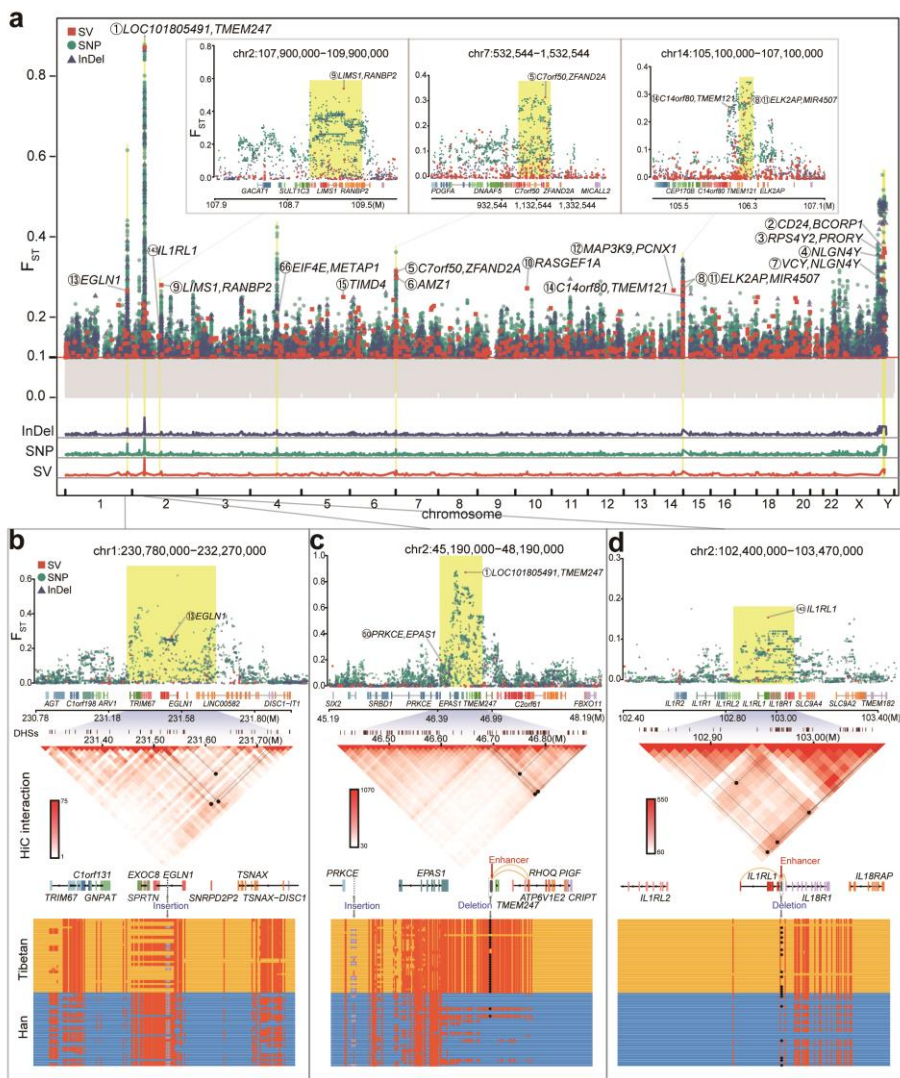


**Figure 4. Comparison of Han-Tibetan populations reveals the genetic landscape of evolutionary adaptation.**

**a.** Manhattan plot (top) based on the FST values of SVs (orange-red boxes), SNPs (blue-green dots) and InDels (dark blue triangles) between the Han and Tibetan cohorts. Overall, 15 SVs with an FST>0.25 are highlighted (yellow), and associated genes are labelled (black) with rank (circled number). The shadows in the Manhattan plot for SVs, SNPs and InDels (bottom) suggest the high consistency of evolutionary selection for SVs, SNPs and InDels. **b.** Manhattan plot (top), TAD (middle) and haplotype (bottom) near EGLN1 on chromosome 1 based on the FST values of SNPs, InDels, and SVs between the Han and Tibetan cohorts. A 131 bp insertion (grey) in the intron of EGLN1 shows high LD with SNPs (red dot) and potentially disrupts a loop (black dot and inverted triangle) boundary. **c.** Manhattan plot (top), TAD (middle) and haplotype (bottom) near EPAS1 and TMEM247 on chromosome 2 based on the FST values of SNPs, InDels, and SVs between the Han and Tibetan cohorts. The most Tibetan-specific deletion disrupts an enhancer (red arrow) targeting (yellow line) ATP6V1E2 and RHOQ; it also potentially disrupts a loop (black dot and inverted triangle) boundary. This region shows an additional 121 bp insertion (purple dot) upstream of EPAS1 and SNPs with high LD, possibly reflecting multiple selective events. **d.** Manhattan plot (top), TAD (middle) and haplotype (bottom) near IL1RL1 on chromosome 2 based on the FST values of SNPs, InDels, and SVs between the Han and Tibetan cohorts. A deletion in the exon of IL1RL1 disrupts an enhancer (red arrow) targeting (yellow line) IL1RL1 and IL18RL1; it also potentially disrupts a loop (black dot and inverted triangle in TAD) boundary.

## 267 SV signals of selection for high-altitude adaptation

268 Several SNPs are linked to the high-altitude adaptation of Tibetans<sup>5,19-21</sup>; however, the studies on the roles that  
269 SVs play in the evolution of Tibetan adaptation to high altitudes are very limited. Therefore, to study the  
270 differences in the Han and Tibetan populations, we first filtered the SVs with an  $F_{ST} > 0.1$ , resulting in 612 SVs.  
271 The TibetanSV webserver (<https://zhilong.shinyapps.io/tibetan>) provides these SVs with associated annotations.  
272 Among these SVs, 319 SVs were novel, not being identified in the 1KPG, gnomAD, dbVar and DGV databases,  
273 and 457 SVs showed a higher frequency in Tibetan people than in Han people. These SVs are candidate high-  
274 altitude adaptation SVs. For example, an insertion was on an intron of *EGLN1* (rank 13, dbsv6981,  $F_{ST}=0.27$ ,  
275 1q42.2), and *EGLN1* is associated with high-altitude, as reported previously<sup>8</sup>. Two intergenic translocations  
276 between *MDH1* and *UGP2* (dbsv66039\_1 and dbsv66040\_1,  $F_{STs}=0.15$ , 2p15) were found in 14% of Tibetans  
277 and zero Han individuals. *MDH1* was found to be among the top 10 evolutionarily selected regions in rhesus  
278 macaques living on a plateau<sup>22</sup>, while *MDG1B*, a parologue of *MDH1*, has been reported to be a target of  
279 selection in Tibetans<sup>4</sup>.

280 SVs exhibit broad and distal regulation through cis-regulatory circuitry rewiring. Among 612 SVs, 61% SVs (373)  
281 overlapped with a promoter, enhancer, silencer, topologically associating domain (TAD) boundary or chromatin  
282 loop boundaries. Overall, 71 deletions (**Supplementary Fig. 4b**) and 29 insertions (**Supplementary Fig. 4c**)  
283 overlapped with enhancers, 19 SVs overlapped with promoters, 9 SVs overlapped with silencers and 347 SVs  
284 were associated with a TAD/loop boundary (see the TibetanSV webserver). For example, one exonic deletion  
285 (dbsv59520,  $F_{ST}=0.15$ , 2q12.1) associated with *IL1RL1* in 45% of Tibetan and 18% of Han individuals resulted  
286 in the truncation of one of the protein-coding transcripts of *IL1RL1* (**Fig. 4d**). This deletion, located within a TAD,  
287 disrupts a loop and an enhancer in lung tissue, affecting *IL18R1* and *IL1RL* through cis-regulatory circuitry  
288 rewiring (**Fig. 4d**). Both *IL1RL1* and *IL18R1* are associated with asthma, a breathing-related lung disease<sup>23</sup>, and  
289 many other immune system diseases. The fact that the prevalence rate of asthma in Tibetan children is lower  
290 than that in Han children indicates that *IL1RL1* could be a target for treating asthma.

291 We chose 15 SVs with an  $F_{ST}>0.25$ , including 6 novel SVs, for an in-depth investigation of the relationship  
292 between the associated genes and the biological traits of Tibetans (**Fig. 5a**). The biological functions and tissue-  
293 specific high expression of the protein-coding genes located near these SVs were visualized in a network (**Fig.**  
294 **5b**). Some of these genes, including *EPAS1*, *CRIP2* and *GNPAT*, are highly expressed in artery, lung and heart  
295 tissues, while others, such as *UNCX*, *ADAM19* and *CYFIP2*, are highly expressed in the blood, and many of the  
296 genes, such as *TTC7A* and *BRAT1*, are highly expressed in the testis. Importantly, these genes are associated  
297 with the response to hypoxia, inflammation, glucose, lipid and energy metabolism, insulin receptor signalling,  
298 blood coagulation and keratin filaments in these tissues, indicating their roles in high-altitude adaptation.

## 299 *EPAS1/TMEM247* SV disrupts a super enhancer

300 The strongest Tibetan-specific signal was found for the dbsv57015 deletion, located on 2p21 (rank 1,  $F_{ST}=0.87$ )  
301 between two hypoxia-related genes, *EPAS1* and *TMEM247*. This deletion was fully linked ( $LD=1$ ) with 212 SNPs  
302 (78 in *EPAS1*, 19 in *TMEM247*) and 17 InDels in 43 Tibetan samples (**Fig. 4c**), indicating a long haplotype  
303 consistent with adaptive selection. Multiple genome-wide association studies (GWASs) have associated these  
304 SNPs with high-altitude adaptation, red blood cell counts, body fat distribution, offspring birth weight, and HDL  
305 cholesterol (**Supplementary Table 9**), consistent with multiple biological adaptations to high altitude. This region  
306 showed an additional insertion (dbsv62730, 2p21,  $F_{ST}=0.20$ ) upstream of *EPAS1* (**Fig. 4c**), possibly reflecting  
307 multiple selective events. Notably, both *EPAS1* and *TMEM247* are also positively selected in Tibetan Mastiff  
308 dogs<sup>24</sup> and show distinct association signals<sup>25</sup>, suggesting that they both functionally contribute to adaptation.  
309 These results suggest that this SV influences high-altitude adaptation collaboratively with these SNPs and InDels.

310 We next sought to understand the specific mechanistic role of the dbsv57015 deletion. This deletion overlapped

311 an enhancer predicted by EpiMap<sup>26</sup> and enhancerDB (vista31415)<sup>27</sup>, indicating a possible gene-regulatory  
312 function. We generated 4 truncated segments of the 3.4 kb deletion-containing sequence of dbsv57015 and  
313 tested each independently in kidney-derived 293T cells. We found that all 4 sequences showed significantly  
314 increased luciferase activity compared to the control (up to 2.3-fold for the first 1 kb segment) (**Fig. 5d**), indicating  
315 that the deleted region plays a *cis*-regulatory role. This deletion also affected the expression of *ATP6V1E2* and  
316 *RHOQ*, both of which are targets of the super enhancer (**Fig. 4c and Supplementary Fig. 4b**). These two genes  
317 are involved in signalling via GPCR and insulin receptor signalling pathways, which play critical roles in the hypoxia  
318 response<sup>28,29</sup>; indeed, both insulin and glucose levels are reduced in Tibetan individuals relative to Han  
319 individuals<sup>30</sup>. These findings indicate gene-regulatory roles of dbsv57015 through the deactivation of a gene-  
320 regulatory enhancer element with combined effects on multiple genes.

### 321 **The sequence of dbsv57015 affects gene transcription activity via *trans*-regulatory circuitry.**

322 A DNA pull-down assay revealed binding proteins including ATP synthase and binding cassette proteins, general  
323 transcription factors and prolyl 4-hydroxylase subunit alpha-1 (P4HA1). Surprisingly, P4HA1 expression is  
324 induced by HIF-1 under hypoxia, P4HA1 can stabilize HIF- 1 $\alpha$ , leading to positive feedback regulation and  
325 increased expression of HIF- 1- induced genes<sup>31</sup>. The binding of P4HA1 indicated a potential role in high-  
326 altitude adaptation. Gene Ontology analysis following the DNA pull-down assay showed that the binding proteins  
327 of the dbsv57015 sequence were mainly enriched in biological processes related to ribonucleoprotein complex  
328 biogenesis and DNA conformation change (**Supplementary Fig. 5 and Supplementary Table 10**). The deletion  
329 of the dbsv57015 sequence in Tibetans also rewires the *trans*-regulatory circuitry by disrupting the binding of  
330 transcription factors within this genomic region, suggesting a compensatory low demand for oxygen under  
331 hypoxia by inhibiting multiple unnecessary molecular and cellular activities. In summary, the most Tibetan-  
332 specific deletion was associated with high-altitude adaptation through complex *cis*- and *trans*-regulatory circuitry  
333 rewiring.

### 334 **Examples of biological roles for specific SVs**

#### 335 **Dbsv104311 is involved in longevity, sleep quality, and emotion in the Tibetan population.**

336 The insertion located between *C7orf50* and *ZFAND2A* (rank 5, dbsv104311,  $F_{ST}=0.31$ , 7p22.3) is accompanied  
337 by 5 additional deletions ( $F_{ST}>0.1$ , TibetanSV webserver), indicating a strong selective signal (**Supplementary Fig.**  
338 **6a**). These deletions fall within a genetic region that has been associated with insomnia symptoms, longevity,  
339 and systolic blood pressure in multiple GWAS (**Supplementary Table 9**). In addition, *ZFAND2A* is associated  
340 with the lifespan of *C. elegans*<sup>32</sup>, shows several SNPs with differential allele frequencies in Tibetan individuals  
341 (**Fig. 5c**) and has been shown to be selected in Tibetan pigs<sup>24</sup>. *C7orf50* was previously associated with  
342 miserableness in a transcriptome-wide association study<sup>33</sup>. Indeed, Tibetan individuals show increased  
343 longevity<sup>34</sup>, reduced agrypnia and insomnia symptoms of acute mountain sickness, and reduced dispiritedness  
344 relative to non plateau-living individuals, indicating that these SVs may contribute to these adaptive phenotypic  
345 differences.

#### 346 **Inflammation plays a key role in the survival in cold, hypoxic environments.**

347 Three Tibetan-specific SVs were found in the same chromosomal segment (14q32.33), including an intergenic  
348 deletion between *ELK2AP* and *MIR4507* (rank 8, dbsv31666,  $F_{ST}=0.27$ ), an intergenic insertion between  
349 *ELK2AP* and *MIR4507* (rank 11, dbsv32695,  $F_{ST}=0.27$ ) and a deletion in the intergenic region between *C14orf80*  
350 and *TMEM121* (rank 14, dbsv31619,  $F_{ST}=0.25$ ) (**Supplementary Fig. 6b**), indicating a strongly selected region.  
351 These SVs are in high LD with multiple SNPs associated with blood protein levels, composite immunoglobulin,  
352 and autoimmune traits (**Supplementary Table 9**), indicating potential roles in blood flow and immunoregulation.  
353 Indeed, Tibetan individuals show significantly higher total protein levels<sup>30</sup> associated with inflammation, which is  
354 an important response to hypoxic cold environments and can mitigate altitude-related illness<sup>35</sup>.

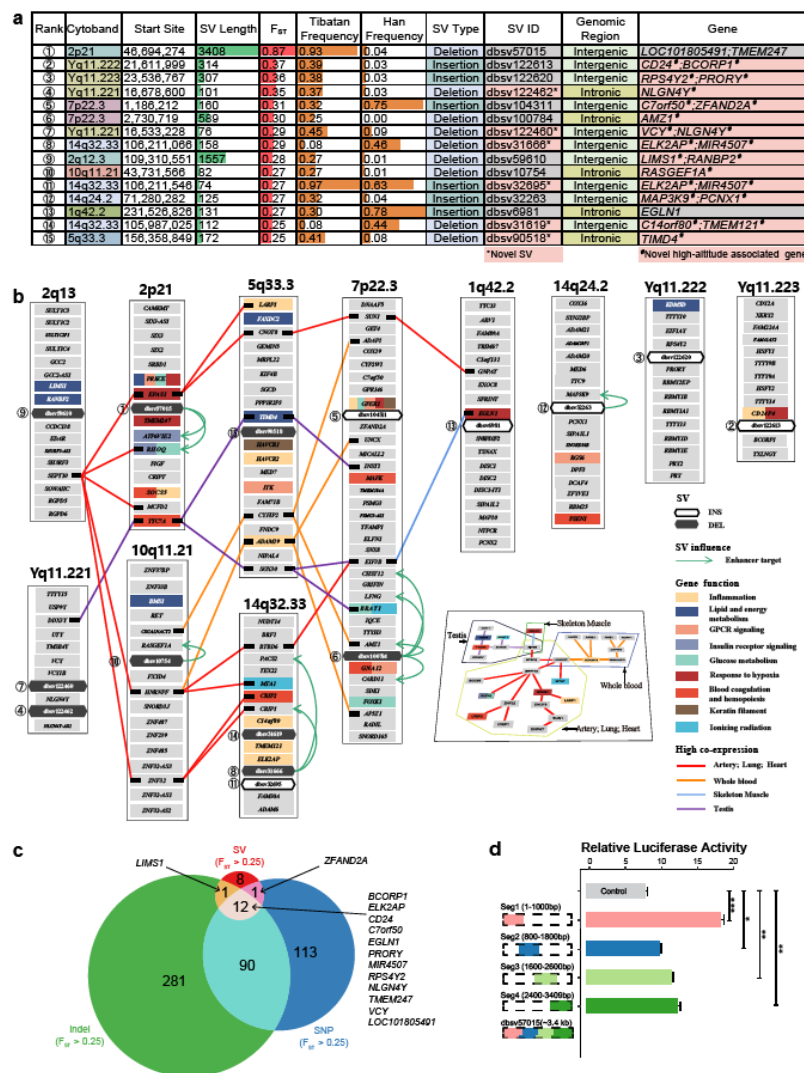


**Figure 5. Evolutionary selection of genes for adaptation to high altitude in Tibetans.** **a.** Basic description of 15 SVs with an FST > 0.25 ordered by FST values. We discovered 6 novel SVs (highlighted in pink in the SV ID column) and 13 novel high-altitude-associated gene groups (highlighted in pink in the Gene column). **b.** The biological functions (coloured rectangles) and tissue-specific high expression (coloured lines) of the protein-coding genes located near the top 15 population-specific SVs (black or white hexagons) are visualized in a network. Most of these genes are related to the response to hypoxia, inflammation, glucose, lipid and energy metabolism, insulin receptor signalling, blood coagulation and keratin filaments in these tissues, indicating their roles in high-altitude adaptation. **c.** Venn diagram of nearby genes related to SNPs, InDels and SVs with an FST > 0.25. The high consistency between the associated genes of SNPs, InDels and SVs indicates coincidental natural selection at high altitudes. The non-overlapping genes suggest special functions of these genomic variations. **d.** Fluorescence intensity comparison for the dbsv57015 deletion and control reporter proves that the deleted sequence is an enhancer. Kidney-derived 293T cells were transfected with the pGL3 control vector, Seg1, Seg2, Seg3 or Seg4 (n=5 per group). The pRL-TK plasmid encoding the Renilla luciferase gene was cotransfected into these cells and used as an internal control for transfection efficiency. Both firefly luciferase and Renilla luciferase activities were sequentially measured 48 h after transfection. \*P < 0.05, \*\*P < 0.01, \*\*\*P < 0.001.

372 **Lipid metabolism supplies additional energy to Tibetans for high-altitude adaptation.**

373 A Tibetan-specific intergenic deletion between *LIMS1* and *RANBP2* (rank 9, dbsv59610,  $F_{ST}=0.28$ , 2q12.3) lies  
374 within a region that is genetically associated with triglycerides and LDL cholesterol levels according to GWAS  
375 (**Supplementary Table 9**). Indeed, Tibetans exhibit lower triglyceride, cholesterol and LDL levels and higher  
376 HDL levels than Han individuals<sup>30</sup>, and they consume more energy generated through lipid metabolism to meet  
377 the energetic needs imposed by hypoxia and low temperatures on Han people living on high-altitude plateaus  
378 relative to Han individuals living on plains. Indeed, genes related to lipid and fat metabolism have also been  
379 associated with high-altitude adaptation in rhesus macaques<sup>22</sup>, indicating convergent metabolic adaptation in  
380 humans and other primates. The above deletion is also associated with excessive hairiness, lobe size, and lung  
381 function (**Supplementary Table 9**), which are traits consistent with high-altitude adaptation.

382 **Several SVs are associated with relieving high-altitude sickness symptoms in Tibetans.**

383 One identified Tibetan-specific deletion was located in an intron of *TIMD4* (rank 15, dbsv90518,  $F_{ST}=0.25$ ,  
384 5q33.3), upstream of *HAVCR1*, a gene associated with headache<sup>36</sup>. This deletion disrupts a predicted enhancer  
385 (enh87362) included in EnhancerDB<sup>27</sup> that is predicted to regulate *TIMD4*. Notably, *HAVCR1* is an important  
386 parologue of *TIMD4*. As headaches and migraines are associated with changes in vascular blood flow to the  
387 brain, this deletion may contribute to the observed differences in headache incidence between Han and Tibetan  
388 individuals at high altitude<sup>37</sup>. This deletion is also associated with triglycerides, LDL cholesterol and total  
389 cholesterol levels (**Supplementary Table 9**), which may provide a mechanistic explanation for these vascular  
390 differences or may indicate pleiotropic effects across multiple pathways.

391 **Multiple SVs show Tibetan-specific functions in traits such as heel bone mineral density and birth weight.**

392 Twelve Tibetan-specific SVs showing an  $F_{ST}>0.1$  were associated with heel bone mineral density, including an  
393 intergenic deletion between *SLC8A1* and *LINC01913* (rank 21, dbsv58385,  $F_{ST}=0.23$ , 7p22.3) and an intronic  
394 deletion in *CNOT4* (rank 28, dbsv103188,  $F_{ST}=0.22$ , 7q33) (**Supplementary Table 9**). An intronic deletion in  
395 *AMZ1* (rank 6, dbsv100784,  $F_{ST}=0.3$ , 7p22.3) disrupts an enhancer whose targets include *AMZ1*, which is  
396 associated with heel bone mineral density according to the GWAS Catalog, possibly contributing to the increase  
397 in tP1NP procollagen<sup>30</sup> and lower prevalence of osteoporosis observed in Tibetans relative to the Han population.

398 Ten identified SVs with an  $F_{ST}>0.1$  are associated with birth weight (**Supplementary Table 9**). Generally, high-  
399 altitude reduces infant birth weight as a result of intrauterine growth restriction; however, the birth weight of  
400 Tibetans is higher than that of Han individuals living at high altitudes<sup>38</sup>.

401 **Other SVs of unclear function that are worth exploring.** Among the 15 SVs with an  $F_{ST}>0.25$ , one intronic  
402 SV and one intergenic SV were associated with *NLGN4Y* (**Supplementary Fig. 6c**), which is related to learning,  
403 vocalization behaviour, presynapse assembly, and autism. Two of the intergenic SVs were associated with  
404 *ELK2AP*, *MIR4507* or *IGHG1* and *IGHG3* according to GENCODE annotation (**Supplementary Fig. 6b**).  
405 *RPS4Y2* (**Supplementary Fig. 6d**) and *RANBP2* (**Supplementary Fig. 6e**) are involved in influenza viral RNA  
406 transcription and replication. Additionally, *RANBP2* is related to the regulation of glucokinase and hexokinase  
407 activity. *CD24* (**Supplementary Fig. 6f**), *MAPK3K9* and *RASGEF1A* are involved in the MAPK cascade.

408 **Gene variations, including SNPs, InDels, and SVs, regulate genes both collectively and independently.**

409 As we found that several peaks in the Manhattan plot of SNPs, InDels, and SVs were highly consistent (**Fig. 4a**),  
410 the collection of SNPs, InDels and SVs with an  $F_{ST}>0.25$  provides a set of perfect candidate genes that may be  
411 involved in the high-altitude adaptation of Tibetans. We obtained overlapping genes between the annotated  
412 genes related to SNPs and InDels with an  $F_{ST}>0.25$ , and 12 of the 22 genes appeared in all 3 gene sets (**Fig.**  
413 **5b**). The overlap between the three call sets verified that most of our identified SVs are associated with high-  
414 altitude adaptation. A total of 382 genes showing an  $F_{ST}$  greater than 0.1 were identified among the genes

415 associated with SVs, SNPs and InDels. Although there were different genes in each set, the overlapping genes  
416 between them indicated that SVs, InDels and SNPs function collectively to support high-altitude adaptation.  
417 However, different types of gene variations were also shown to exhibit specific functions when considering non-  
418 overlapping genes. This suggests both cooperative and independent contributions of SVs, SNPs, and InDels in  
419 high-altitude adaptation. More generally, gene variations, consisting of SNPs, InDels, and SVs, function both  
420 collectively and independently to regulate genes in human biology.

421 **Denisovan-introgressed SVs were not selected during the evolution of the Tibetan genome.** We also  
422 identified several ancient SVs that existed in apes or ancient hominins (**Supplementary Fig. 7**). For example,  
423 the *EGLN1*-related insertion (rank 13, dbsv6981,  $F_{ST}=0.27$ , 1q42.2) was identified from apes; a duplication in the  
424 exonic *HLA-DRB5* (rank37, dbsv99370,  $F_{ST}=0.22$ , 6p21.32) was identified in Denisovans and did not exist in  
425 apes, Africans, or Neanderthals. Notably, no SVs with high  $F_{ST}$  values were discovered in ancient hominins,  
426 although a 5-SNP motif in *EPAS1* introgressed from Denisovans contributed to the high-altitude adaptation of  
427 Tibetans.

#### 428 Functional significance of SVs in evolutionary adaptation

429 The high-altitude environment shapes the fat metabolism, steroid hormone production, heart functions, and brain  
430 development of Tibetans to allow them survive on the plateau. Beyond these individual examples, we searched  
431 for systematic genome-wide enrichment of our Tibetan (**Supplementary Fig. 8a**) and Han (**Supplementary Fig.**  
432 **8b**) SVs in specific pathways through KEGG<sup>39</sup> analysis, excluding singleton SVs. We found that Tibetan-specific  
433 SVs were enriched in multiple key metabolic pathways, consistent with the adaptive advantages of Tibetans in  
434 cold and hypoxic environments, including those related to steroid hormone biosynthesis and fat digestion and  
435 absorption, which can be helpful for producing sufficient body heat and energy in cold environments. We also  
436 observed enrichment related to vascular function, pulmonary function, blood pressure, and vascular smooth  
437 muscle contraction, which can play important roles in adaptation to hypoxic conditions. We observed enrichment  
438 in alpha-linolenic acid metabolic pathways, which are known to reduce the risk of coronary heart disease and  
439 improve cardiovascular health. We found strong enrichment of the herpes simplex virus 1 infection pathway,  
440 consistent with the fact that the prevalence and incidence of herpes simplex virus 1 infections are relatively  
441 higher in the Western Pacific<sup>40</sup>, likely reflecting a historic prevalence of viral infections. We also found notable  
442 enrichment of several Gene Ontology<sup>41</sup> terms. These terms were related to synapse assembly and organization,  
443 cognition, and learning or memory processes (enriched in Tibetan-specific SVs with an  $F_{ST}>0.1$ ) and several  
444 immune processes, including T cell activation (enriched in Han-specific SVs with an  $F_{ST}>0.1$  (**Supplementary**  
445 **Fig. 8c**). These genes also showed enrichment related to specific Gene Ontology terms related to cellular  
446 components, including synaptic localization (**Supplementary Fig. 8d**), consistent with observed differences in  
447 cognitive pathways. These broad biological enrichment results indicate that high-altitude adaptation involves  
448 multiple biological pathways related to metabolism, vasculature, circulation, and cognition allowing survival in  
449 cold, hypoxic environments.

#### 450 Discussion

451 Our study provides an important high-resolution view of the high-altitude adaptation of Tibetans based on the  
452 long-read sequencing of 320 Han and Tibetan genomes, revealing the complex SV landscape of Han and  
453 Tibetan populations, and we further obtained important insights for understanding the evolutionary adaptation of  
454 the Tibetan population through a systematic study of the genomic SV landscape. We provide 122,876 high-  
455 quality Han and Tibetan SVs, dramatically expanding the known landscape of genetic variation and the  
456 corresponding resources available for East Asian populations. We revealed many candidate SVs and genes for  
457 high-altitude adaptation, revealing diverse biological adaptations consistent with the observed physiological  
458 differences in the Tibetan population. The most Tibetan-specific SV has a broad impact on gene regulation via

459 complex *cis*- and *trans*-regulatory circuits. Different types of genomic variations, consisting of SNPs, InDels, and  
460 SVs, function both in combination and in parallel.

461 The understanding of the human genome is changing dramatically with continuing technological developments.  
462 The NGS of large cohorts has revealed the important roles of genomic variations in the evolutionary adaptation  
463 of human populations. Our long-read ONT-based study provides the first large SV reference panel based on a  
464 cohort of 320 Han and Tibetan individuals. Quality evaluation of our SV call sets through comparisons between  
465 our SV call set and those of the 1KGP and gnomAD, comparisons between ONT and CCS SV call sets from the  
466 same sample, and qPCR validation confirmed the high quality of this call set. It fills a gap in lower EAS-based  
467 genetic resources for community studies, as reported previously. Our study further confirmed the high  
468 enrichment of SVs in genomic repeat regions. We also found hotspots of SVs in the genome and showed an  
469 evolutionary preference for repeat regions associated with intronic SVs. All these results reveal a prospective  
470 landscape of high genetic diversity and complexity for human genomic variations and evolution.

471 We systematically assessed the SV landscape of Han and Tibetan populations. The Han and Tibetan  
472 populations could be separated by PCA and admixture analysis based only on the SV call set. This situation has  
473 previously been demonstrated through SNP analysis<sup>4</sup>. This finding demonstrated that SVs can be considered  
474 functionally equal to SNPs to some extent. SVs and their impacts on human health and diseases are worthy of  
475 broad, in-depth studies. We compared the SVs between Han and Tibetan populations and identified SVs with  
476 high  $F_{ST}$  values, which are probably related to high-altitude adaptation. Several of these SVs are related to known  
477 hypoxia-associated genes, while most of them were have not been previously identified in high-altitude  
478 environments, and six of the SVs were novel. These findings proved the value of the ONT resequencing of the  
479 Han and Tibetan populations. Our results provide a great resource for the identification of candidate genes for  
480 high-altitude adaptation.

481 The selection observed among SNPs, InDels, and SVs was highly consistent between the Tibetan and Han  
482 populations. By comparing genes related to SNPs, InDels, and SVs with high  $F_{ST}$  values between the Han and  
483 Tibetan populations, we found that some genes were simultaneously associated with the three types of gene  
484 variation. This provides a strong signal that these genes are involved in high-altitude adaptation. There were  
485 also some genes that were associated with only one or two types of gene variation. Different types of gene  
486 variation function both in combination and in parallel to achieve perfect adaptation to the plateau environment.

487 We found that SVs show wide and distal regulation through *cis*- and *trans*-regulatory circuitry rewiring. A majority  
488 of the SVs with an  $F_{ST} > 0.1$  overlapped with *cis*-regulatory elements. An *IL1RL1*-associated exonic deletion  
489 disrupts an exon of *IL1RL1* and the enhancer, suggesting the disruption of this gene and *cis*-regulatory circuitry  
490 rewiring. Multiple SVs, including the most Tibetan-specific SVs and an *EGLN1*-associated SV, disrupt a TAD or  
491 loop boundary, affecting the *cis*-regulatory circuitry. We used an enhancer reporter assay and a DNA pull-down  
492 assay to show that the strongest Tibetan-specific SV ( $F_{ST}=0.87$ ) is associated with a complex *cis*- and *trans*-  
493 regulatory circuit, resulting in the deletion of a super enhancer bound by several key transcription factors and  
494 targeting multiple nearby genes through proximal and distal interactions, illustrating the role of non-exonic SVs  
495 in gene-regulatory circuitry rewiring.

496 We provide several dramatic examples of adaptation related to the hypoxia response, red blood cell count, blood  
497 pressure, body fat distribution, birth weight, bone mineral density, energy and lipid metabolism, insomnia,  
498 agrypnia, longevity, mountain sickness, immunoregulation, inflammation, lung function, brain vascular blood flow,  
499 and headache. These examples illustrate the broad set of biological processes involved in high-altitude  
500 adaptation, the biological relevance of our findings, and the power of our integrative genomics approach for  
501 revealing the biological processes involved in adaptive events.

502 Overall, our study demonstrates the power of single-molecule long-read sequencing, provides an important  
503 greatly expanded comprehensive reference for global SVs, reveals many dramatic biological examples of human  
504 adaptation, provides important biological targets for combatting hypoxia, illustrates complex gene-regulatory  
505 circuitry rewiring mediated by SVs, and provides a wealth of biological insights into human biology and recent  
506 human adaptation.

507 **Figure Legends**

508 **Figure 1. SV discovery in 119 Tibetan and 201 Han samples**

509 a. Summary of the experimental pipeline. Overall, 320 Han and Tibetan samples were collected and sequenced  
510 via the ONT platform, resulting in 122,876 SVs. Candidate SVs for high-altitude adaptation, their functional  
511 regulatory mechanisms based on their connections with exons, enhancers and TAD boundaries, and  
512 candidate genes for high-altitude adaptation were explored. *Cis*- and *trans*-regulatory circuitry rewiring was  
513 validated in two biological assays.

514 b. The numbers of 5 types of SVs in Han, Tibetan, and all samples. The majority are deletions and insertions.

515 c. Allele frequency consistency between the SVs in the Han and Tibetan cohort and the 1KGP EAS cohort. The  
516 high consistency between them indicates the high quality of our SV call set.

517 d. GC content distribution of insertions and deletions in the Han and Tibetan cohort and the EAS cohort,  
518 indicating that the ONT platform performs well even in genomic regions with a biased GC content.

519 e. Overlap between the SVs of our cohort and 1KGP and gnomAD cohorts, showing 83,094 novel SVs.

520 f. Overlap between the SVs of our cohort and the 1KGP EAS cohort, showing a 6-fold increase in the number  
521 of previously annotated East Asian SVs.

522 **Figure 2. SV composition, length frequency, and chromosome distributions**

523 a. SV proportions in different genome regions. The majority of SVs are associated within repeat elements, such  
524 as LINEs and SINEs as shown in the pie chart.

525 b. Densities of repeats and their-associated SVs, all SVs, regulatory elements and genes in the genome. There  
526 are hotspots (peaks with red arrow) of SVs in the genome.

527 c. Correlations between repeat elements, their-associated SVs, regulatory elements and genes in the genome.  
528 Different types of SVs are highly positively (red) inter-correlated. High correlation coefficients are boxed (red  
529 for positive and blue for negative).

530 **Figure 3. Population genetics of Han-Tibetan populations**

531 a. PCA of the SV call sets of the Tibetan and Han cohorts and 1KGP African (AFR), American (AMR), East  
532 Asian (EAS), European (EUR) and South Asian (SAS) cohorts. The Han (red) and Tibetan (green) populations  
533 are close to the EAS (brown) populations, as expected, and can be clearly separated according to PC3 and  
534 PC6.

535 b. Population structure of the Tibetan and Han populations. Admixture analysis (top), clustered SVs with an  
536  $F_{ST} > 0.1$  (bottom). The SVs can distinguish two populations, although the number of SVs per individual in the  
537 two populations is similar.

538 c. A clear separation between Han and Tibetan with 3 sample exception in the evolutionary tree analysis based  
539 on all the SVs of Han (red) and Tibetan (green).

540 **Figure 4. Comparison of Han-Tibetan populations reveals the genetic landscape of evolutionary adaptation.**

541 a. Manhattan plot (top) based on the  $F_{ST}$  values of SVs (orange-red boxes), SNPs (blue-green dots) and InDels  
542 (dark blue triangles) between the Han and Tibetan cohorts. Overall, 15 SVs with an  $F_{ST} > 0.25$  are highlighted  
543 (yellow), and associated genes are labelled (black) with rank (circled number). The shadows in the  
544 Manhattan plot for SVs, SNPs and InDels (bottom) suggest the high consistency of evolutionary selection

545 for SVs, SNPs and InDels.

546 b. Manhattan plot (top), TAD (middle) and haplotype (bottom) near *EGLN1* on chromosome 1 based on the  
547  $F_{ST}$  values of SNPs, InDels, and SVs between the Han and Tibetan cohorts. A 131 bp insertion (grey) in the  
548 intron of *EGLN1* shows high LD with SNPs (red dot) and potentially disrupts a loop (black dot and inverted  
549 triangle) boundary.

550 c. Manhattan plot (top), TAD (middle) and haplotype (bottom) near *EPAS1* and *TMEM247* on chromosome 2  
551 based on the  $F_{ST}$  values of SNPs, InDels, and SVs between the Han and Tibetan cohorts. The most Tibetan-  
552 specific deletion disrupts an enhancer (red arrow) targeting (yellow line) *ATP6V1E2* and *RHOQ*; it also  
553 potentially disrupts a loop (black dot and inverted triangle) boundary. This region shows an additional 121  
554 bp insertion (purple dot) upstream of *EPAS1* and SNPs with high LD, possibly reflecting multiple selective  
555 events.

556 d. Manhattan plot (top), TAD (middle) and haplotype (bottom) near *IL1RL1* on chromosome 2 based on the  
557  $F_{ST}$  values of SNPs, InDels, and SVs between the Han and Tibetan cohorts. A deletion in the exon of *IL1RL1*  
558 disrupts an enhancer (red arrow) targeting (yellow line) *IL1RL1* and *IL18RL1*; it also potentially disrupts a  
559 loop (black dot and inverted triangle in TAD) boundary.

560 **Figure 5. Evolutionary selection of genes for adaptation to high altitude in Tibetans.**

561 a. Basic description of 15 SVs with an  $F_{ST}>0.25$  ordered by  $F_{ST}$  values. We discovered 6 novel SVs (highlighted  
562 in pink in the SV ID column) and 13 novel high-altitude-associated gene groups (highlighted in pink in the  
563 Gene column).

564 b. The biological functions (coloured rectangles) and tissue-specific high expression (coloured lines) of the  
565 protein-coding genes located near the top 15 population-specific SVs (black or white hexagons) are  
566 visualized in a network. Most of these genes are related to the response to hypoxia, inflammation, glucose,  
567 lipid and energy metabolism, insulin receptor signalling, blood coagulation and keratin filaments in these  
568 tissues, indicating their roles in high-altitude adaptation.

569 c. Venn diagram of nearby genes related to SNPs, InDels and SVs with an  $F_{ST}>0.25$ . The high consistency  
570 between the associated genes of SNPs, InDels and SVs indicates coincidental natural selection at high  
571 altitudes. The non-overlapping genes suggest special functions of these genomic variations.

572 d. Fluorescence intensity comparison for the dbsv57015 deletion and control reporter proves that the deleted  
573 sequence is an enhancer. Kidney-derived 293T cells were transfected with the pGL3 control vector, Seg1,  
574 Seg2, Seg3 or Seg4 (n=5 per group). The pRL-TK plasmid encoding the Renilla luciferase gene was  
575 cotransfected into these cells and used as an internal control for transfection efficiency. Both firefly luciferase  
576 and Renilla luciferase activities were sequentially measured 48 h after transfection. \*P<0.05, \*\*P<0.01, \*\*\*  
577 P<0.001.

578 **Supplementary figure legends**

579 **Supplementary Figure 1. Han & Tibetan SV call set.** (a) The number distribution of each type of SVs in Han  
580 and Tibetan samples. (b) The cumulative percentage of the number of SVs excluding singletons within the  
581 Tibetan cohort. (c) The cumulative percentage of the number of SVs excluding singletons within the Han cohort.  
582 (d) The cumulative percentage of the number of SVs excluding singletons within the Han and Tibetan cohort. (e)  
583 Venn diagram between the Han and Tibetan SV call set and the SVs identified based on 15 publicly available  
584 genomes generated by long-read sequencing. (f) Venn diagrams of the overlap among the Han and Tibetan,  
585 1KGP, gnomAD and 15 genome SV call sets.

586 **Supplementary Figure 2. Characteristics of SV distribution and composition.** (a) Frequencies of different  
587 types of SVs with lengths shorter than 1 kb. The length of Alu is approximately 300 bp. (b) Frequencies of

588 different types of SVs with lengths longer than 1 kb. The length of LINEs is approximately 6 kb. (c) The numbers  
589 of 5 types of SVs in different gene elements. (d) The proportions of SINE- and LINE-mediated SVs and exonic  
590 SVs in different types of SVs. (e) The frequencies of SVs and the proportions of all SVs. (f) Overall, 58 SVs are  
591 associated with C7orf50. (g) The ratio between repeat-associated SVs and non-repeat associated SVs among  
592 singleton, all and shared SVs. (h) The percentages of different gene elements related to singleton, all and shared  
593 SVs in the Han and Tibetan populations. (i) The percentages of 5 types of SVs related to singleton, all and  
594 shared SVs in the Han and Tibetan populations.

595 **Supplementary Figure 3. Population genetics of Han and Tibetan populations.** (a) Overlap between the  
596 SVs in Han and Tibetan populations, showing that they share a majority of SVs. (b) PCA of the SV call set of the  
597 Tibetan (green) and Han (red) cohorts indicates clear separation between the two groups.

598 **Supplementary Figure 4. Chromosome landscape of Han-Tibetan population and related enhancers.** (a)  
599 Manhattan plot for each chromosome based on the  $F_{ST}$  values (y-axis) of SVs (orange-red boxes), SNPs (blue  
600 green dots) and InDels (dark blue triangles) between the Han and Tibetan cohorts. (b) The SVIDs of deletions  
601 and genes targeted by enhancers (y-axis) are connected (red) with different enhancers in different tissues (x-  
602 axis). (c) The SVIDs of insertions and genes targeted by enhancers (y-axis) are connected (red) with different  
603 enhancers in different tissues (x-axis).

604 **Supplementary Figure 5. DNA pull-down results for the dbsv57015 sequence.** (a) The sequence of  
605 dbsv57015 consists of T1 and T2. (b) Venn diagram of pulled-down proteins in the 293T cell line. (c) Gene  
606 Ontology (GO) biological process enrichment of the proteins in the control and pull-down groups in the 293T cell  
607 line. (d) Venn diagram of pulled-down proteins in the U266 cell line. (e) GO biological process enrichment of the  
608 proteins in the control and pull-down groups in the U266 cell line.

609 **Supplementary Figure 6. Manhattan plot of several population-specific genomic regions.** (a) Manhattan  
610 plot of the region near the *ZFAND2A* gene based on the  $F_{ST}$  values of SVs, SNPs and InDels between the Han  
611 and Tibetan cohorts. (b) Manhattan plot near gene *ELK2AP* based on the  $F_{ST}$  of SV, SNP and InDel between the  
612 Han and Tibetan cohorts. (c) Manhattan plot of the region near the *NLGN4Y* gene based on the  $F_{ST}$  values of  
613 SVs, SNPs and InDels between the Han and Tibetan cohorts. (d) Manhattan plot of the region near the *PRS4Y2*  
614 gene based on the  $F_{ST}$  values of SVs, SNPs and InDels between the Han and Tibetan cohorts. (e) Manhattan  
615 plot of the region near the *RANBP2* gene based on the  $F_{ST}$  values of SVs, SNPs and InDels between the Han  
616 and Tibetan cohorts. (f) Manhattan plot of the region near the *CD24* gene based on the  $F_{ST}$  values of SVs, SNPs  
617 and InDels between the Han and Tibetan cohorts.

618 **Supplementary Figure 7. Possible evolutionary scenarios of SVs.** The numbers of SVs are shown under  
619 each scenario. In addition, a majority of SVs existed only in the Tibetan and Han populations.

620 **Supplementary Figure 8. Enrichment analysis of Han/Tibetan-specific SVs.** (a) Top 10 KEGG pathways of  
621 Tibetan-specific SVs, excluding singleton SVs. (b) Top 10 KEGG pathways of Han-specific SVs, excluding  
622 singleton SVs. (c) Gene Ontology (GO) biological process enrichment terms for Han-specific or Tibetan-specific  
623 SVs with an  $F_{ST}>0.1$ . (d) GO cellular component enrichment terms of Han-specific or Tibetan-specific SVs with  
624 an  $F_{ST}>0.1$ .

## 625 Supplementary Table legends

626 **Supplementary Table 1.** (a) Samples and ONT sequencing statistical information. (b) Manual curation  
627 of 298 SVs across all samples. (c) PCR validation of 4 SVs in 57 samples. (d) Statistics of SMRT-CCS  
628 sequencing data. (e) The number and frequency of different gene elements and types of SVs among  
629 singleton, shared and all SVs. (f) Samples and NGS statistical information.

630 **Supplementary Table 2.** Statistics of ONT and SMRT-CCS sequencing data.

631 **Supplementary Table 3.** Orthogonal validation of ONT-SVs against SMRT-CCS-SVs from the same

632 sample.

633 **Supplementary Table 4.** AF distribution of different types of novel SVs in the Tibetan-Han population.

634 **Supplementary Table 5.** SV comparison between ZF1 and our Tibetan population data.

635 **Supplementary Table 6.** Mean SV statistics for each sample of different AFs in the Tibetan-Han

636 population.

637 **Supplementary Table 7.** SV distribution in different genomic regions in the Tibetan-Han population.

638 **Supplementary Table 8.** SINE- and LINE-associated SVs in various genomic functional regions.

639 **Supplementary Table 9.** SV-SNP-GWAS-phenotype analysis results.

640 **Supplementary Table 10.** Proteins identified and their annotation in DNA pull-down assays of the

641 sequence of the most Tibetan-specific SVs.

642 **Method details**

643 **Key resources table**

Software/Algorithms	Source	Website
Guppy (2.0.10)	Oxford Nanopore Technologies	<a href="https://community.nanoporetech.com">https://community.nanoporetech.com</a>
NGMLR (0.2.7)	Sedlazeck et al. 2018	<a href="https://github.com/philres/ngmlr">https://github.com/philres/ngmlr</a>
Sniffles (1.0.8)	Sedlazeck et al. 2018	<a href="https://github.com/fritzsedlazeck/Sniffles">https://github.com/fritzsedlazeck/Sniffles</a>
SMRTLink (6.0)	Pacific Biosciences, 2018	<a href="https://www.pacb.com/support/documentation/?fwp_asset_type=release-notes&amp;fwp_sort=preserve">https://www.pacb.com/support/documentation/?fwp_asset_type=release-notes&amp;fwp_sort=preserve</a>
pbsv (2.4.0)	Wenger et al. 2019	<a href="https://github.com/PacificBiosciences/pbsv">https://github.com/PacificBiosciences/pbsv</a>
FALCON (1.8.7)	Chin et al. 2016	<a href="https://github.com/PacificBiosciences/FALCON">https://github.com/PacificBiosciences/FALCON</a>
dbSVmerge	GrandOomics	<a href="https://github.com/GrandOomics/svmerge">https://github.com/GrandOomics/svmerge</a>
Plink (1.9)	Purcell et al. 2007	<a href="http://www.cog-genomics.org/plink2/">http://www.cog-genomics.org/plink2/</a>
frappe (1.1_linux64)	Tang et al. 2005	<a href="https://med.stanford.edu/tanglab/software/frappe.html">https://med.stanford.edu/tanglab/software/frappe.html</a>
vcftools (0.1.17)	Danecek et al. 2011	<a href="http://vcftools.sourceforge.net/downloads.html">http://vcftools.sourceforge.net/downloads.html</a>
SVhawkeye	This paper	<a href="https://github.com/yywan0913/SVhawkeye">https://github.com/yywan0913/SVhawkeye</a>
bwa (0.7.17-r1188)	Li. 2013	<a href="https://github.com/lh3/bwa">https://github.com/lh3/bwa</a>

Pindel (0.2.5b8)	Ye et al. 2009	<a href="https://github.com/genome/pindel">https://github.com/genome/pindel</a>
Delly (0.7.9)	Rausch et al. 2012	<a href="https://github.com/dellytools/delly">https://github.com/dellytools/delly</a>
Truvari	English. 2018	<a href="https://github.com/spiralgenetics/truvari">https://github.com/spiralgenetics/truvari</a>
HiC-Pro (2.11.1)	Servant et al. 2015	<a href="http://github.com/nservant/HiC-Pro">http://github.com/nservant/HiC-Pro</a>
fastp (0.12.6)	Chen et al. 2018	<a href="https://github.com/OpenGene/fastp">https://github.com/OpenGene/fastp</a>
cworld-dekker (0.0.1)	Miura et al. 2018	<a href="https://github.com/dekkerlab/cworld-dekker">https://github.com/dekkerlab/cworld-dekker</a>
Bowtie2 (2.3.2)	Langmead and Salzberg, 2012	<a href="https://sourceforge.net/projects/bowtie-bio/files/bowtie2/2.3.2/">https://sourceforge.net/projects/bowtie-bio/files/bowtie2/2.3.2/</a>
Picard (V2.5.0)	Li, H. et al. 2010.	<a href="http://broadinstitute.github.io/picard/">http://broadinstitute.github.io/picard/</a>
GATK (v3.3.0)	McKenna, A. et al. 2010.	<a href="https://software.broadinstitute.org/gatk/">https://software.broadinstitute.org/gatk/</a>
SnpEff	Cingolani P. et al. 2012.	<a href="http://snpeff.sourceforge.net/">http://snpeff.sourceforge.net/</a>
CNVnator	Abyzov A. et al. 2011.	<a href="https://omictools.com/cnvnator-tool">https://omictools.com/cnvnator-tool</a>
Breakdancer	Fan X, et al. 2014.	<a href="http://breakdancer.sourceforge.net/">http://breakdancer.sourceforge.net/</a>
SIFT	Ng P C, et al. 2003.	<a href="https://sift.bii.a-star.edu.sg/">https://sift.bii.a-star.edu.sg/</a>
MutationTaster	Schwarz J M, et al. 2010.	<a href="http://www.mutationtaster.org/">http://www.mutationtaster.org/</a>
PolyPhen2	Ivan Adzhubei, et al. 2013.	<a href="http://genetics.bwh.harvard.edu/pph2/">http://genetics.bwh.harvard.edu/pph2/</a>
Condel	Yuan X, et al. 2018.	<a href="https://omictools.com/condel-tool">https://omictools.com/condel-tool</a>
FATHMM	Shihab HA, et al. 2013.	<a href="http://fathmm.biocompute.org.uk/">http://fathmm.biocompute.org.uk/</a>
Public Data		
hg19	NCBI	<a href="ftp://ftp-trace.ncbi.nih.gov/1000_genomes/ftp/technical/reference/human_g1k_v37.fasta.gz">ftp://ftp-trace.ncbi.nih.gov/1000_genomes/ftp/technical/reference/human_g1k_v37.fasta.gz</a>
1000 Genome Project	1000 Genomes Project Consortium	<a href="https://doi.org/10.1038/nature15393">https://doi.org/10.1038/nature15393</a>
gnomAD (2.1.1)	Karczewski et al., 2019	<a href="https://gnomad.broadinstitute.org/">https://gnomad.broadinstitute.org/</a>

dbVar	NCBI	<a href="https://www.ncbi.nlm.nih.gov/dbvar">https://www.ncbi.nlm.nih.gov/dbvar</a>
TibetanSV webserver	This paper	<a href="https://zhilong.shinyapps.io/tibetan">https://zhilong.shinyapps.io/tibetan</a>
segdup	UCSC Genome browser	<a href="http://hgdownload.cse.ucsc.edu/goldenPath/hg19/database/genomicSuperDups.txt.gz">http://hgdownload.cse.ucsc.edu/goldenPath/hg19/database/genomicSuperDups.txt.gz</a>
rmsk	UCSC Genome browser	<a href="http://hgdownload.cse.ucsc.edu/goldenPath/hg19/database/rmsk.txt.gz">http://hgdownload.cse.ucsc.edu/goldenPath/hg19/database/rmsk.txt.gz</a>
Dgv (2016-05-15)	Database of Genomic Variants	<a href="http://dgv.tcag.ca/">http://dgv.tcag.ca/</a>
Decipher (Version3)	DatabasE of genomiC varlation and Phenotype in Humans using Ensembl Resources	<a href="https://decipher.sanger.ac.uk/about/downloads/documents">https://decipher.sanger.ac.uk/about/downloads/documents</a>
OMIM	Online Mendelian Inheritance in Man	<a href="https://omim.org/downloads">https://omim.org/downloads</a>
ANNOVAR (17 Jul 2017)	Wang et al. 2010	<a href="https://annovar.openbioinformatics.org/en/latest/user-guide/download/">https://annovar.openbioinformatics.org/en/latest/user-guide/download/</a>
Promoter	FANTOM5 Human Promoters	<a href="http://slidebase.binf.ku.dk/human_promoters/bed">http://slidebase.binf.ku.dk/human_promoters/bed</a>
Enhancer	Epimap Repository	<a href="https://personal.broadinstitute.org/cboix/epimap/links/links_corr_only/">https://personal.broadinstitute.org/cboix/epimap/links/links_corr_only/</a>
Silencer	SilencerDB	<a href="http://health.tsinghua.edu.cn/silencerdb/download.php">http://health.tsinghua.edu.cn/silencerdb/download.php</a>
HiC TAD, Loop	3D Genome Browser	<a href="http://3dgenome.fsm.northwestern.edu/">http://3dgenome.fsm.northwestern.edu/</a>
Phenotype	GWAS Catalog	<a href="https://www.ebi.ac.uk/gwas/downloads">https://www.ebi.ac.uk/gwas/downloads</a>
Fifteen human genome SVs	Audano et al. 2019	<a href="http://ftp.1000genomes.ebi.ac.uk/vol1/ftp/data_collections/hgsv_sv_discvery/working/20181025_EEE_SV-Pop_1">http://ftp.1000genomes.ebi.ac.uk/vol1/ftp/data_collections/hgsv_sv_discvery/working/20181025_EEE_SV-Pop_1</a>
ZF1	Ouzhuluobu et al. 2019	<a href="https://doi.org/10.1093/nsr/nwz160">https://doi.org/10.1093/nsr/nwz160</a>
Denisovan	Meyer et al. 2012	<a href="https://doi.org/10.1126/science.1224344">https://doi.org/10.1126/science.1224344</a>
Neandertal	Prüfer et al. 2014	<a href="https://doi.org/10.1038/nature12886">https://doi.org/10.1038/nature12886</a>
Ust' Ishim	Fu et al. 2014	<a href="https://doi.org/10.1038/nature13810">https://doi.org/10.1038/nature13810</a>

644

## 645 Samples and third-generation sequencing

646 To ensure that we covered the majority of SVs that were shared within or among the Han or Tibetan  
 647 populations, we sequenced 201 Han and 119 Tibetan genomes based on ONT sequencing. All the

648 samples were selected randomly (**Table S1**). We oversampled Han genomes by sequencing more  
649 individual Han genomes than Tibetan genomes because we anticipated finding more diverse SVs in  
650 the Han population, which shows high admixture relative to the Tibetan population.

651 Genomic DNA was prepared from each of the 320 samples by sodium dodecyl sulphate (SDS)-based  
652 methods. Then, nanopore libraries were constructed according to the manufacturer's instructions for  
653 the Ligation Sequencing Kit 1D (SQK-LSK109) and sequenced on R9.4 flow cells using a PromethION  
654 sequencer (ONT, UK) at the Genome Center of Grandomics (Beijing, China). Base calling was  
655 subsequently performed from fast5 files using Guppy (v2.0.10) software to generate the FASTQ files.

656 To compare the results of SV calling with those of the other long-read sequencing platform, one of the  
657 Tibetan samples, AL-2-33, was randomly selected for sequencing on the PacBio Sequel system. The  
658 genomic DNA was sheared, and size selection of 10-15 kb fragments was performed by using  
659 BluePippin (Sage Science, USA). SMRTbell libraries were constructed using the SMRTbell Template  
660 Prep Kit v.1.0 (100-259-100, PacBio) and then sequenced using V3.0 chemistry on the PacBio Sequel  
661 system. CCS reads were generated using SMRTLink (v6.0) software from PacBio.

#### 662 SV calling

663 To produce high-quality reference SV sets for the Han and Tibetan populations, we constructed a  
664 stringent analysis workflow. The complete sequencing and analysis workflow consisted of 1) an  
665 average sequencing depth of  $20.85 \pm 7.54X$  with a long read length (average N50 length= $22.71 \pm 4.04$   
666 kb) (**Table S1A**); 2) SV calling by using Sniffles, which has been proven to be the most effective  
667 computational tool for identifying SVs from nanopore sequencing data thus far<sup>13</sup>; 3) the orthogonal  
668 validation of ONT-SVs against SMRT-CCS-SVs using 453.79 Gb of total polymerase bases, which  
669 produces CCS data with a 15.4X depth (**Table S1D**); 4) the manual curation of 95,360 SVs from 298  
670 candidate regions (**Table S1B**) that were originally mapped by the computational pipeline; 5) the  
671 selection of 228 SVs (**Table S1C**) for validation using PCR and Sanger sequencing; and 6) the cross-  
672 comparison of our SVs with those in various human genome variant databases and those reported in  
673 recently published work. The FASTQ files were aligned to the hg19 human reference genome available  
674 from NCBI, and a BAM format alignment file was produced using NGMLR v0.2.7<sup>13</sup> with default  
675 parameters, which is designed for long-read mapping. Variants were called using Sniffles v1.0.8<sup>13</sup> with  
676 the parameter setting -q 0 -l 50 --report\_BND, and VCF format files were generated, which contained  
677 all SV information. Then, raw SVs were filtered and merged to obtain high-quality SVs. The two filtering  
678 criteria were that the AF needed to be greater than 0.3 and that the sequencing depth of the variant  
679 had to be greater than the larger number between 0.3-fold and 2-fold the average sequencing depth  
680 and less than the twice the average sequencing depth. High-quality SVs were used for the subsequent  
681 analysis. The SVs derived from PacBio and ONT sequencing platforms were compared according to  
682 the following criterion:  $50 \text{ bp} \leq \text{SV length} \leq 50,000 \text{ bp}$ , using Truvari.

#### 683 SV annotation and distributions

684 High-quality SVs with upstream and downstream genes were annotated in the segdup, rmsk,.dgv, 1000  
685 Genome Project, gnomAD, Decipher, OMIM, and ANNOVAR databases. We grouped the SVs into 500  
686 kb bins to count the number of various types of SVs (insertions, duplications, deletions, inversions, and

687 translocations). The cytoband file was downloaded from the UCSC website, and chromosome banding  
688 was drawn for different regions. The numbers of SVs indicated in different colours were determined  
689 using the R language 3.4.1<sup>42</sup>.

#### 690 SV merging

691 DbSVmerge was used to obtain the nonredundant SV set for all high-quality SVs from 320 samples.  
692 The merging strategy was as follows: the distance of the variant coordinates between any two SVs  
693 must be less than 1 kb; for deletion-, duplication- and inversion-type SVs, at least 40% of the region  
694 should overlap; and for insertion SVs, the difference in length between insertions should be less than  
695 twice the length of both insertions. The numbers and lengths of SVs of different types (insertions,  
696 duplications, deletions, inversions, and translocations) were counted.

#### 697 SVs comparison among published datasets

698 We compared our SV calls to several published datasets, including the 1KGP dataset<sup>43</sup>, gnomAD 2.1.1,  
699 SVs from fifteen human genome sequences obtained on PacBio platforms [8], and Tibetan ZF1 SVs<sup>16</sup>.  
700 The same merging strategy was applied using dbSVmerge. The SV comparison was conducted with  
701 Truvari according to the following criterion: 50≤ SV length ≤50,000.

#### 702 SV landscape in Tibetan and Han Chinese populations

703 We constructed nonredundant sets of 93,154 SVs from 119 samples from the Tibetan population and  
704 109,438 SVs from 201 samples from the Han Chinese population. In this study, SV frequency (also  
705 called allele frequency (AF)) was defined as the proportion of the sample size with one SV in the  
706 population (calculated excluding singletons). To determine whether the sample size was large enough  
707 for SV population analysis, we drew curves of SV counts among samples as every sample was added  
708 to the population.

709 We divided AFs into 5 levels: 0~0.1, 0.1~0.4, 0.4~1, and 1. SV numbers were counted according to the  
710 5 levels and the singletons in each individual. Then, the diversity of the SVs in repeat and nonrepeat  
711 regions was quantified for different types of SVs.

#### 712 Genome evolution analysis using SVs

713 Each SV was given a value of 1 if someone had it and 0 if not, resulting in an N×M matrix, where N  
714 stands for the number of samples (320) and M represents the total number of all SVs. All PCAs,  
715 evolutionary trees, and population structure analyses were based on the N×M matrix. PCA was carried  
716 out and the principal component values were calculated with the R 3.4.1 prcomp function, ensuring that  
717 fewer principle components were reserved than the number of samples. Hierarchical clustering was  
718 included for plotting the evolutionary tree using the R 3.4.1 hcluster function. Population genetic  
719 structure analysis can reveal the time span of the development of subgroups by dividing a large  
720 population into several subgroups. Plink<sup>44</sup> software in two modes, pep and map, was utilized to obtain  
721 structural information statistics for each individual, which were analysed with Frappe software<sup>45</sup>.

#### 722 Short-read sequencing, SNP and InDel calling

723 Short-read sequencing of 148 samples (75 Tibetan and 73 Han, including 113 DNA samples (previously  
724 used for ONT sequencing) and 35 blood samples) was performed after a series of sample and library

725 processing steps. A Qubit Fluorometer was used to evaluate the concentration of DNA, and agarose  
726 gel electrophoresis was used to examine sample integrity and purity. Fragmented DNA was obtained  
727 through Covaris preparation and subjected to selection at an average size of 200-400 bp using an  
728 Agencourt AMPure XP-Medium kit. The PCR-amplified products were recovered with the AxyPrep Mag  
729 PCR clean up kit.

730 We performed the paired-end sequencing of the 148 samples with an average output of 137 Gb raw  
731 bases. Each sample showed a read depth >31.9X. To reduce sequencing noise, we removed reads  
732 containing a) 10% or more 'N' bases, b) 50% or more low-quality bases, or c) sequencing adapters.  
733 After data filtering, we applied Burrows-Wheeler Aligner (BWA v0.7.12) to map the clean reads against  
734 the hg19 human reference genome. We sorted the mapping results and marked duplicate reads in  
735 BAM files using Picard tools (v1.118). We performed base quality score recalibration (BQSR) and local  
736 realignment around InDels to obtain a more accurate base quality and therefore improve the accuracy  
737 of the variant calls. We detected SNPs and small InDels using HaplotypeCaller from the Genome  
738 Analysis Toolkit (GATK, v3.3.0). We further applied variant quality score recalibration (VQSR), a variant  
739 filtering tool based on the machine learning method, to obtain reliable variant calls with high confidence.

#### 740 Analysis of adaptive evolution using SVs

741  $F_{ST}$  measures population differentiation due to genetic structure using the SV frequency, calculated as  
742 the difference between total heterozygosity and average population heterozygosity divided by total  
743 heterozygosity. The heterozygosity frequency of SVs between populations was calculated by Weir and  
744 Cockerham estimators using the statistical method of VCFtools<sup>46</sup>.

745 Tibetan-specific SVs were selected on the basis of satisfying three criteria: the population frequency in  
746 Tibetans was not less than 0.2, the population frequency in Tibetans was twice as high as that in Han  
747 individuals, and the  $F_{ST}$  of the SV was larger than 0.1. Han-specific SVs were obtained using a similar  
748 strategy: the population frequency in the Han population should be not less than 0.2, the population  
749 frequency in the Han population should be twice that in the Tibetan population, and the  $F_{ST}$  of SV should  
750 be larger than 0.1. Some population-specific SVs were examined manually with IGV<sup>47</sup>.

751 Raw data, either FASTQ or BAM files, for Denisovan<sup>48</sup>, Altai Neandertal<sup>49</sup>, Vindija Neandertal<sup>50</sup> and  
752 Ust' Ishim genomes<sup>51</sup> were downloaded from the European Nucleotide Archive. We aligned the archaic  
753 short reads to the hg19 human reference genome using BWA-MEM<sup>52</sup>. For each archaic hominin  
754 genome, we applied Pindel<sup>53</sup> and Delly<sup>54</sup> to detect SVs and merged the results from the two SV callers  
755 using SURVIVOR<sup>55</sup>.

756 The SV call set from great ape genomes was downloaded from the Database of Genomic Variants  
757 archive (accession number estd235). We converted the coordinates of SVs from reference genome  
758 hg38 to hg19 with the modified open-source tool CrossMap<sup>56</sup>. We applied dbSVmerge to merge all of  
759 these SV call sets with our own SV call set to determine whether an SV was shared between two  
760 genomes or groups/species.

#### 761 LD and GWAS computation

762 To explore the possible connections between different variations (SV and SNP, InDel), the VCF results

763 of 113 samples that were matched with ONT sequencing samples and the VCF results of 320 SVs  
764 were used. The PLINK program was applied to compute the linkage disequilibrium value (LD,  $R^2$ ).  $R^2$   
765 values were computed between SVs and SNPs (InDels) within a window of 1 M bp. The cut-off was set  
766 as 0.2. To annotate the functions of SVs according to SNPs found to be associated with various  
767 phenotypes through GWASs, we made use of the NHGRI Catalog of published GWASs, which includes  
768 159,203 SNPs linked to a multitude of phenotypes. Finally, 1,632 SVs were shown to be in strong LD  
769 ( $R^2 \geq 0.8$ ) with a GWAS SNP found in Han populations, and 1455 SVs were in strong LD ( $R^2 \geq 0.8$ ) with  
770 a GWAS SNP found in Tibetan populations.

### 771 The associations between SV, promoter, silencer, enhancers and HiC data

772 We downloaded gene-enhancer link data from 833 samples in the Epimap Repository<sup>26</sup>. To provide  
773 some tolerance, we extended the breakpoints of 612 SVs ( $F_{ST} > 0.1$ ) by +/-100 bp. We intersected these  
774 SV regions with enhancer regions in each sample. Overall, 100 SV regions showing overlap with at  
775 least one enhancer in any sample were visualized in a heatmap.

776 We analysed the associations between SVs and promoters, silencers, and LADs/TADs/loops in a  
777 similar way. The promoter data were downloaded from FANTOM5 Human Promoters, and the silencer  
778 data were downloaded from SilencerDB. LAD domain data were downloaded from Roadmap, and  
779 TAD/Loop data were obtained from the 3D Genome Browser.

### 780 Pathway and co-expression annotation

781 We selected the 15 SVs with an  $F_{ST} > 0.25$  and identified the ten upstream and downstream genes of  
782 these SVs (excluding noncoding genes) using the GENCODE v29 GRCh37 gff file. According to the  
783 TPM data of these genes in the GTEx database (V8 release), we chose the top ten genes that were  
784 highly expressed in the heart, artery, lung, testis, and whole blood as the genes showing high  
785 coexpression in the tissue. To illustrate the relationships between these genes and high-altitude  
786 adaptation, we chose the GWAS Catalog, SuperPath (<https://pathcards.genecards.org/>), Gene  
787 Ontology, and KEGG databases to annotate the functions of these genes. The clusterProfiler<sup>57</sup> package  
788 was used to enrich pathways.

### 789 Statistical analysis

790 All statistical analyses were performed using the R package (v3.4.1, <http://www.r-project.org/>).

### 791 Dual-luciferase reporter gene assay to validate the function of the dbsv57015 sequence

792 We employed a dual-luciferase reporter gene assay to investigate whether the 3.4 kb dbsv57015  
793 deletion plays a role as a cis-element. For this reason, the four truncated sequences representing  
794 different base pair truncations (Seg1: 1-1000 bp; Seg2: 1600-2400 bp; Seg3: 2600-3409 bp; Seg4:  
795 800-1800 bp) were cloned into the pGL3-control plasmid (Promega, Madison, WI, USA), upstream of  
796 the SV40 promoter and the firefly luciferase reporter gene. A 200-base pair overlap sequence between  
797 two truncated sequences was designed to avoid the disruption of an enhancer, as the core length of  
798 an enhancer is approximately 100-200 bp. These truncated TED-luciferase plasmids were transfected  
799 into 293T cells. Additionally, the pRL-TK vector (Promega, Madison, WI, USA), encoding Renilla  
800 luciferase, was cotransfected in combination with dbsv57015-luciferase reporters as an internal control.  
801 Both firefly luciferase and Renilla luciferase activities were sequentially measured 48 h after  
802 transfection. Firefly luciferase activity was normalized to Renilla luciferase for each sample.

### 803 **DNA pull-down assay to identify the trans-acting regulators of the dbsv57015 sequence**

804 The DNA sequence of dbsv57015 was separated into two parts: T1 (1-1725 bp) and T2 (1676-3409  
805 bp). T1 and T2 DNA probes were affixed to streptavidin magnetic beads (Beaver Biosciences Inc. China)  
806 and then incubated with 293T and U266B1 cell lysates at 4°C overnight. We washed the beads on a  
807 magnetic rack with buffers containing nonspecific DNA and a low salt concentration (50 mmol/L Tris-  
808 HCl, pH 7.6), which removed nonadhering and low-specificity DNA-binding proteins. Then, we washed  
809 the beads with higher salt concentrations (100 mmol/L Tris-HCl, pH 8.5) to elute specific DNA-binding  
810 proteins, which were used to perform sodium dodecyl sulphate polyacrylamide gel electrophoresis.  
811 Silver-stained protein bands corresponding to blank beads (control) and T1 and T2 DNA sequences  
812 were used for mass spectrometry analysis.

### 813 **Data availability**

814 The SV dataset supporting the conclusions of this article is available in the Genome Sequence Archive  
815 repository as accession PRJCA004371(GVM000124, GVM000125) upon acceptance. The data  
816 utilization has an ethical filing number from the Human Genetic Resource Administration of China  
817 (2020BAT0405). The study was approved by the Medical Ethical Committee of Chinese PLA General  
818 Hospital (Beijing, China, S2018-298-02).

### 819 **Acknowledgements**

820 The work was partly supported by the National International Science & Technology Cooperation Special  
821 Program [2013DFA31170] and the Science and Technology program of Beijing [Z151100003915075].  
822 We thank the volunteers who donated samples for this meaningful study. We thank the strong support  
823 from Prof. Tian Yaping, Wang Weidong. We also thank all the participants who contributed to this study.  
824 We thank all the professional comments and suggestions from Ming Ni at Beijing Institute of Radiation  
825 Medicine, Qiang Qiu at Northwestern Polytechnical University, Dongdong Wu at Kunming Institute of  
826 Zoology, Rasmus Nielsen at UC Berkeley, Asan at BGI-Shenzhen.

### 827 **Author contributions**

828 Conceptualization, K.He; Methodology, K.He, J.Shi., Zh.Jia, J.Sun and F.Liang; Study participants  
829 recruitment, X.Zhao, J.Shi., Zh.Jia and Q.Jia; Sample collection and preparation: X.Zhao, J.Shi., Zh.Jia,  
830 Q.Jia, K.Yu, Sh.Wu, S.Cui, Q.Zhong and J.Wu; Data generation and analysis, Zh.Jia, J.Shi., J.Sun,  
831 F.Liang, Ch.Zhao, Depeng Wang, Y.Xiao, Y.Liu and Zh.Wu; Annotation and Functional Links: K.He,  
832 M.P, J.Shi., Zh.Jia, J.Sun, Ch.Zhao, X.Song and Q.Chen; Experimental Validation: K.He, M.P, X.Wang  
833 and Zh.Jia; Writing and revision: J.Shi, Zh.Jia, M.P, F.Liang, M.K., X.Bo and Zh.Wu; Ethics application  
834 and data resource: K.He, J.Shi, K.Yu and X.Zhao; Supervision, K.He.

### 835 **Competing interests**

836 We declare no potential conflicts of interests.

### 837 **References**

1. Spielmann, M., Lupiáñez, D. G. & Mundlos, S. Structural variation in the 3D genome. *Nat. Rev. Genet.* **19**, 453–467 (2018).
2. Laugsch, M. *et al.* Modeling the Pathological Long-Range Regulatory Effects of Human Structural Variation with Patient-Specific hiPSCs. *Cell Stem Cell* **24**, 736–752.e12 (2019).
3. Perry, G. H. *et al.* Diet and the evolution of human amylase gene copy number variation. *Nat. Genet.* **39**, 1256–1260

843 (2007).

844 4. Yi, X. *et al.* Sequencing of 50 human exomes reveals adaptation to high altitude. *Science* **329**, 75–78 (2010).

845 5. Lorenzo, F. R. *et al.* A genetic mechanism for Tibetan high-altitude adaptation. *Nat. Genet.* **46**, 951–956 (2014).

846 6. Huerta-Sánchez, E. *et al.* Altitude adaptation in Tibetans caused by introgression of Denisovan-like DNA. *Nature* **512**,  
847 194–197 (2014).

848 7. Chen, F. *et al.* A late Middle Pleistocene Denisovan mandible from the Tibetan Plateau. *Nature* **569**, 409–412 (2019).

849 8. Simonson, T. S. *et al.* Genetic evidence for high-altitude adaptation in Tibet. *Science* **329**, 72–75 (2010).

850 9. Genetics for all. *Nat. Genet.* **51**, 579 (2019).

851 10. Audano, P. A. *et al.* Characterizing the Major Structural Variant Alleles of the Human Genome. *Cell* **176**, 663–  
852 675.e19 (2019).

853 11. Rishishwar, L., Tellez Villa, C. E. & Jordan, I. K. Transposable element polymorphisms recapitulate human evolution.  
854 *Mob. DNA* **6**, 21 (2015).

855 12. Lin, Y.-L. & Gokcumen, O. Fine-Scale Characterization of Genomic Structural Variation in the Human Genome  
856 Reveals Adaptive and Biomedically Relevant Hotspots. *Genome Biol. Evol.* **11**, 1136–1151 (2019).

857 13. Sedlazeck, F. J. *et al.* Accurate detection of complex structural variations using single-molecule sequencing. *Nat.*  
858 *Methods* **15**, 461–468 (2018).

859 14. Sudmant, P. H. *et al.* An integrated map of structural variation in 2,504 human genomes. *Nature* **526**, 75–81 (2015).

860 15. Collins, R. L. *et al.* A structural variation reference for medical and population genetics. *Nature* **581**, 444–451 (2020).

861 16. He, Y. *et al.* De novo assembly of a Tibetan genome and identification of novel structural variants associated with  
862 high-altitude adaptation. *Natl. Sci. Rev.* **7**, 391–402 (2020).

863 17. Sultana, T. *et al.* The Landscape of L1 Retrotransposons in the Human Genome Is Shaped by Pre-insertion  
864 Sequence Biases and Post-insertion Selection. *Mol. Cell* **74**, 555–570.e7 (2019).

865 18. Weckselblatt, B. & Rudd, M. K. Human Structural Variation: Mechanisms of Chromosome Rearrangements. *Trends*  
866 *Genet.* **31**, 587–599 (2015).

867 19. Xu, S. *et al.* A genome-wide search for signals of high-altitude adaptation in Tibetans. *Mol. Biol. Evol.* **28**, 1003–1011  
868 (2011).

869 20. Petousi, N. & Robbins, P. A. Human adaptation to the hypoxia of high altitude: the Tibetan paradigm from the  
870 pregenomic to the postgenomic era. *J. Appl. Physiol.* **116**, 875–884 (2014).

871 21. Peng, Y. *et al.* Genetic variations in Tibetan populations and high-altitude adaptation at the Himalayas. *Mol. Biol.*  
872 *Evol.* **28**, 1075–1081 (2011).

873 22. Szpiech, Z. A., Novak, T. E., Bailey, N. P. & Stevison, L. S. High-altitude adaptation in rhesus macaques.  
874 doi:10.1101/2020.05.19.104380.

875 23. Grotenboer, N. S., Ketelaar, M. E., Koppelman, G. H. & Nawijn, M. C. Decoding asthma: translating genetic variation  
876 in IL33 and IL1RL1 into disease pathophysiology. *J. Allergy Clin. Immunol.* **131**, 856–865 (2013).

877 24. Wu, D.-D. *et al.* Convergent genomic signatures of high-altitude adaptation among domestic mammals. *Natl Sci Rev*  
878 **7**, 952–963 (2019).

879 25. Deng, L. *et al.* Prioritizing natural-selection signals from the deep-sequencing genomic data suggests multi-variant  
880 adaptation in Tibetan highlanders. *Natl Sci Rev* **6**, 1201–1222 (2019).

881 26. Boix, C. A., James, B. T., Park, Y. P., Meuleman, W. & Kellis, M. Regulatory genomic circuitry of human disease loci  
882 by integrative epigenomics. *Nature* (2021) doi:10.1038/s41586-020-03145-z.

883 27. Kang, R. *et al.* EnhancerDB: a resource of transcriptional regulation in the context of enhancers. *Database* **2019**,  
884 (2019).

885 28. Chakraborty, R., Sikarwar, A. S., Hinton, M., Dakshinamurti, S. & Chelikani, P. Characterization of GPCR signaling in  
886 hypoxia. *Methods Cell Biol.* **142**, 101–110 (2017).

887 29. Ding, D. *et al.* Genetic variation in PTPN1 contributes to metabolic adaptation to high-altitude hypoxia in Tibetan  
888 migratory locusts. *Nat. Commun.* **9**, 4991 (2018).

889 30. Jia, Z. *et al.* Impacts of the Plateau Environment on the Gut Microbiota and Blood Clinical Indexes in Han and Tibetan  
890 Individuals. *mSystems* **5**, (2020).

891 31. Eriksson, J. *et al.* Prolyl 4- hydroxylase subunit alpha 1 (P4HA1) is a biomarker of poor prognosis in primary  
892 melanomas, and its depletion inhibits melanoma cell invasion and disrupts tumor blood vessel walls. *Molecular*

893      Oncology vol. 14 742–762 (2020).

894      32. Yun, C. *et al.* Proteasomal adaptation to environmental stress links resistance to proteotoxicity with longevity in  
895      *Caenorhabditis elegans*. *Proc. Natl. Acad. Sci. U. S. A.* **105**, 7094–7099 (2008).

896      33. Liao, C. *et al.* Multi-tissue probabilistic fine-mapping of transcriptome-wide association study identifies cis-regulated  
897      genes for miserableness. doi:10.1101/682633.

898      34. Li, Y. *et al.* Hypoxia potentially promotes Tibetan longevity. *Cell Res.* **27**, 302–305 (2017).

899      35. Zhou, Y. *et al.* Hypoxia augments LPS-induced inflammation and triggers high altitude cerebral edema in mice. *Brain*  
900      *Behav. Immun.* **64**, 266–275 (2017).

901      36. Lachmann, A. *et al.* Geneshot: search engine for ranking genes from arbitrary text queries. *Nucleic Acids Res.* **47**,  
902      W571–W577 (2019).

903      37. Jiang, C. *et al.* Chronic mountain sickness in Chinese Han males who migrated to the Qinghai-Tibetan plateau:  
904      application and evaluation of diagnostic criteria for chronic mountain sickness. *BMC Public Health* **14**, 701 (2014).

905      38. Moore, L. G., Zamudio, S., Zhuang, J., Sun, S. & Droma, T. Oxygen transport in tibetan women during pregnancy at  
906      3,658 m. *Am. J. Phys. Anthropol.* **114**, 42–53 (2001).

907      39. Kanehisa, M., Furumichi, M., Tanabe, M., Sato, Y. & Morishima, K. KEGG: new perspectives on genomes, pathways,  
908      diseases and drugs. *Nucleic Acids Res.* **45**, D353–D361 (2017).

909      40. James, C. *et al.* Herpes simplex virus: global infection prevalence and incidence estimates, 2016. *Bull. World Health*  
910      *Organ.* **98**, 315–329 (2020).

911      41. The Gene Ontology Consortium. The Gene Ontology Resource: 20 years and still GOing strong. *Nucleic Acids Res.*  
912      **47**, D330–D338 (2019).

913      42. Ihaka, R. & Gentleman, R. R: A Language for Data Analysis and Graphics. *J. Comput. Graph. Stat.* **5**, 299–314  
914      (1996).

915      43. 1000 Genomes Project Consortium *et al.* A global reference for human genetic variation. *Nature* **526**, 68–74 (2015).

916      44. Purcell, S. *et al.* PLINK: a tool set for whole-genome association and population-based linkage analyses. *Am. J. Hum.*  
917      *Genet.* **81**, 559–575 (2007).

918      45. Tang, H., Peng, J., Wang, P. & Risch, N. J. Estimation of individual admixture: analytical and study design  
919      considerations. *Genet. Epidemiol.* **28**, 289–301 (2005).

920      46. Danecek, P. *et al.* The variant call format and VCFtools. *Bioinformatics* **27**, 2156–2158 (2011).

921      47. Robinson, J. T. *et al.* Integrative genomics viewer. *Nat. Biotechnol.* **29**, 24–26 (2011).

922      48. Meyer, M. *et al.* A high-coverage genome sequence from an archaic Denisovan individual. *Science* **338**, 222–226  
923      (2012).

924      49. Prüfer, K. *et al.* The complete genome sequence of a Neanderthal from the Altai Mountains. *Nature* **505**, 43–49  
925      (2014).

926      50. Prüfer, K. *et al.* A high-coverage Neandertal genome from Vindija Cave in Croatia. *Science* **358**, 655–658 (2017).

927      51. Fu, Q. *et al.* Genome sequence of a 45,000-year-old modern human from western Siberia. *Nature* **514**, 445–449  
928      (2014).

929      52. Li, H. Aligning sequence reads, clone sequences and assembly contigs with BWA-MEM. *arXiv [q-bio.GN]* (2013).

930      53. Ye, K., Schulz, M. H., Long, Q., Apweiler, R. & Ning, Z. Pindel: a pattern growth approach to detect break points of  
931      large deletions and medium sized insertions from paired-end short reads. *Bioinformatics* **25**, 2865–2871 (2009).

932      54. Rausch, T. *et al.* DELLY: structural variant discovery by integrated paired-end and split-read analysis. *Bioinformatics*  
933      **28**, i333–i339 (2012).

934      55. Jeffares, D. C. *et al.* Transient structural variations have strong effects on quantitative traits and reproductive isolation  
935      in fission yeast. *Nat. Commun.* **8**, 14061 (2017).

936      56. Zhao, H. *et al.* CrossMap: a versatile tool for coordinate conversion between genome assemblies. *Bioinformatics* **30**,  
937      1006–1007 (2014).

938      57. Yu, G., Wang, L.-G., Han, Y. & He, Q.-Y. clusterProfiler: an R package for comparing biological themes among gene  
939      clusters. *OMICS* **16**, 284–287 (2012).

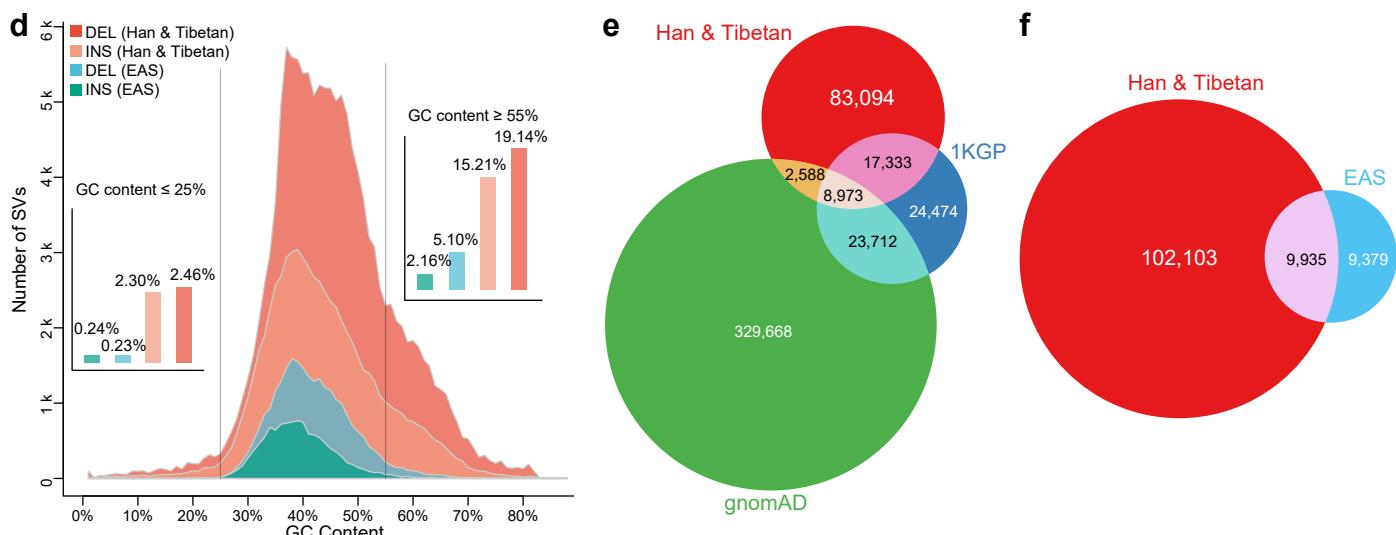
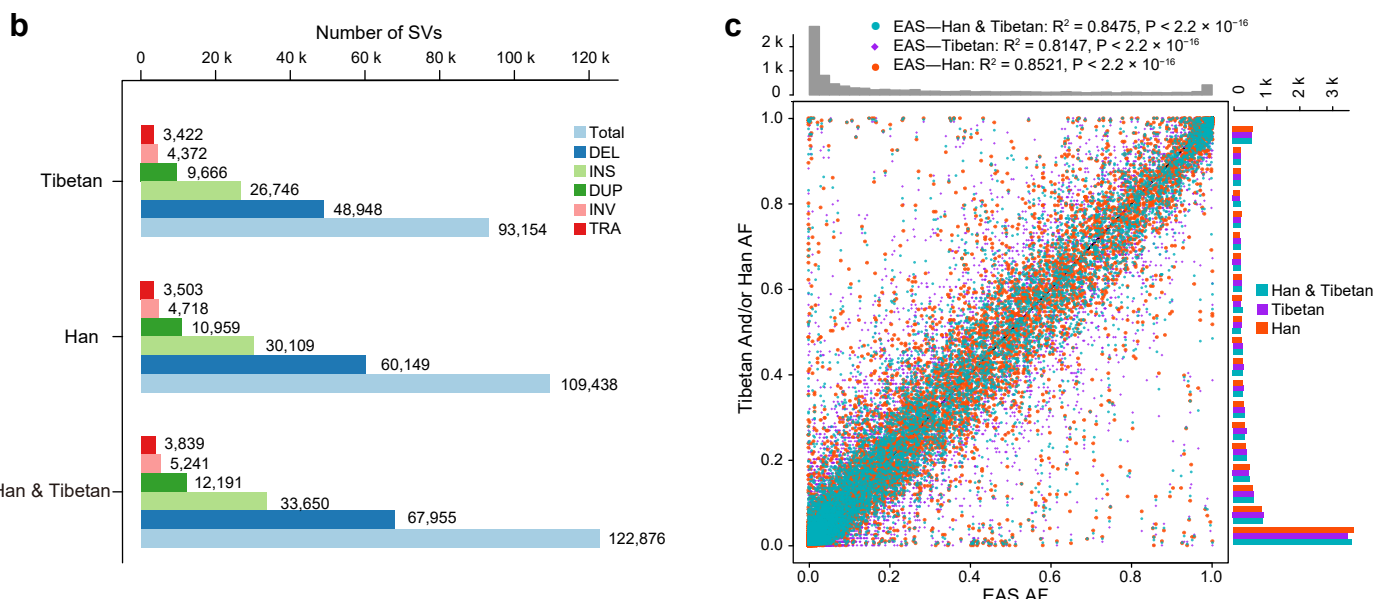
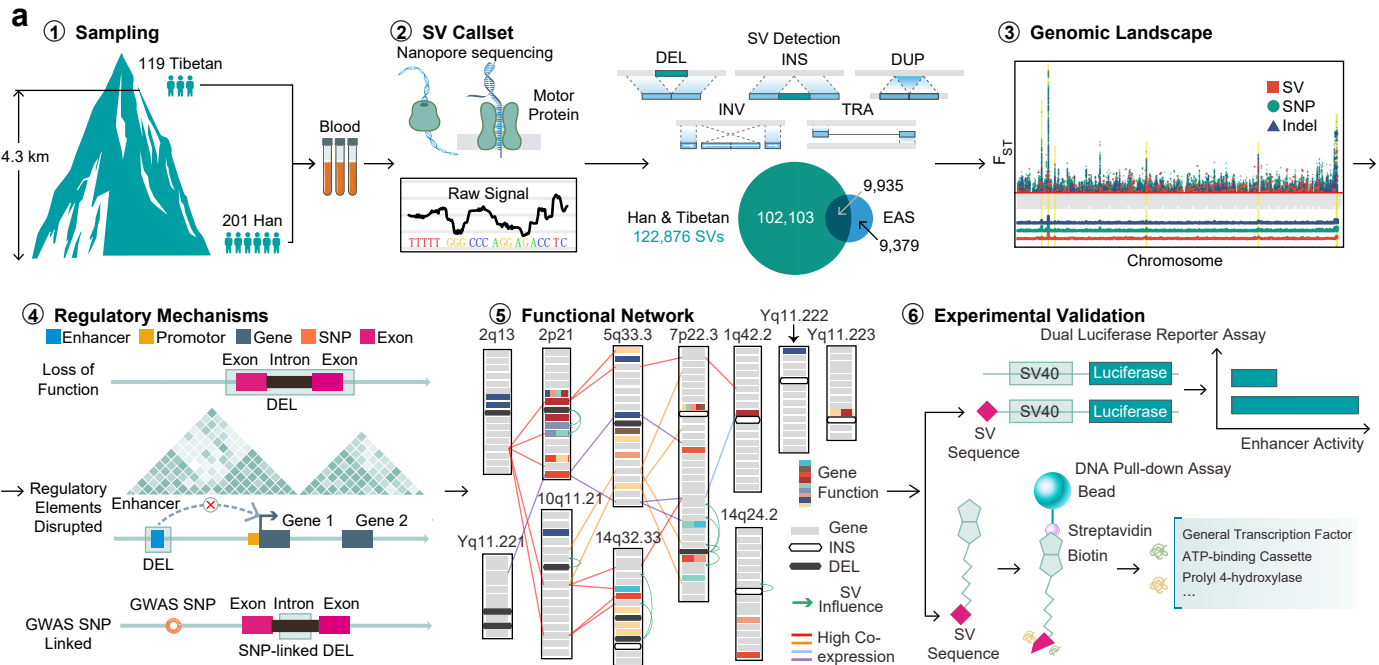


**Figure 1. SV discovery in 119 Tibetan and 201 Han samples.**

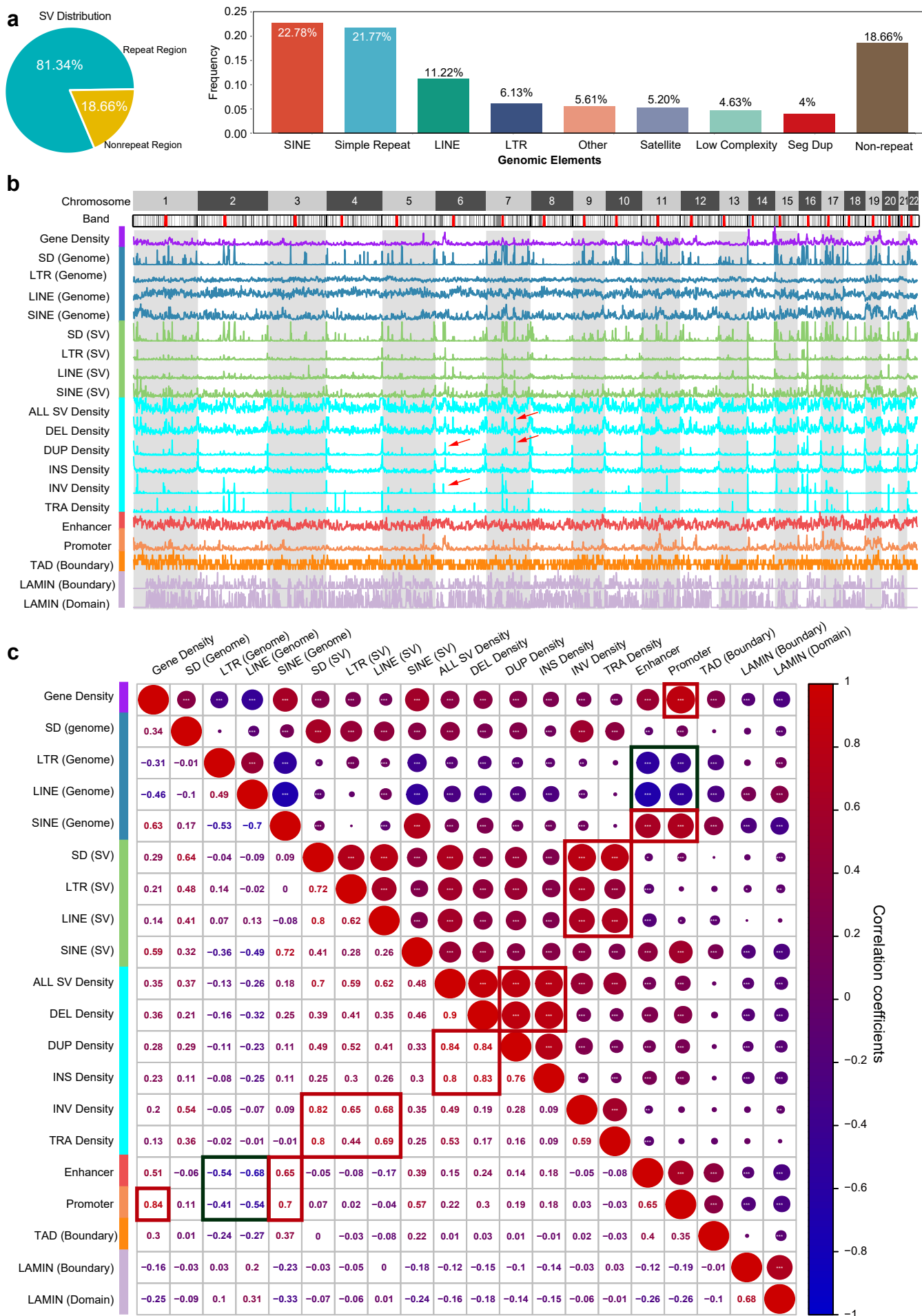
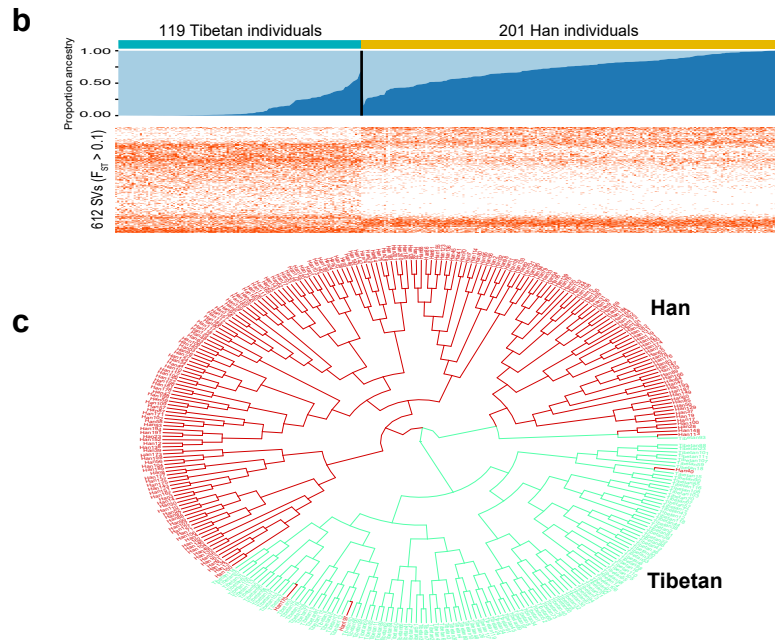
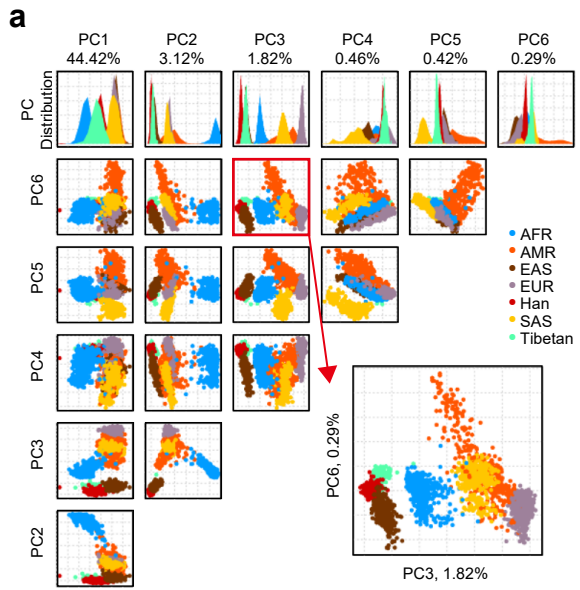
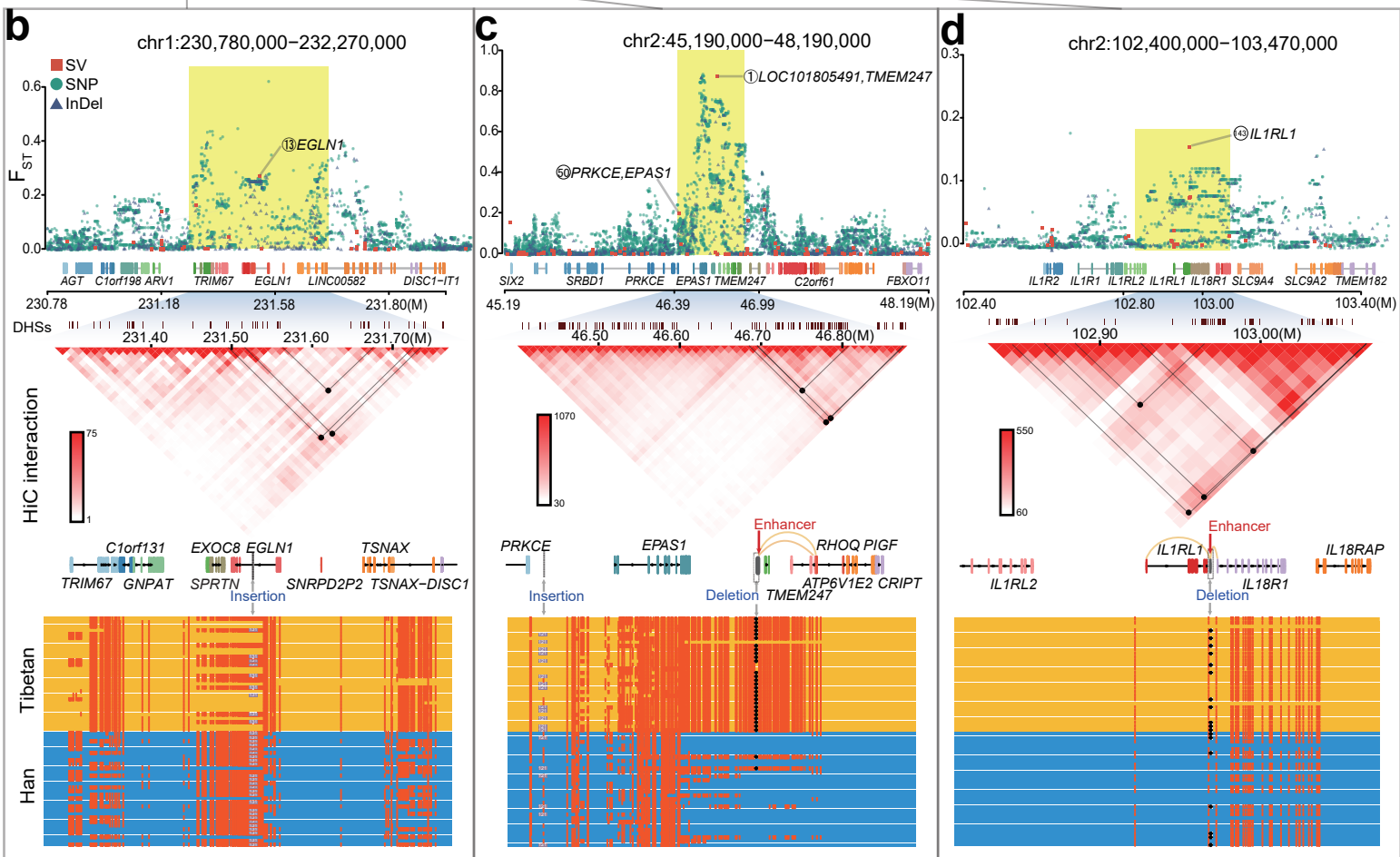
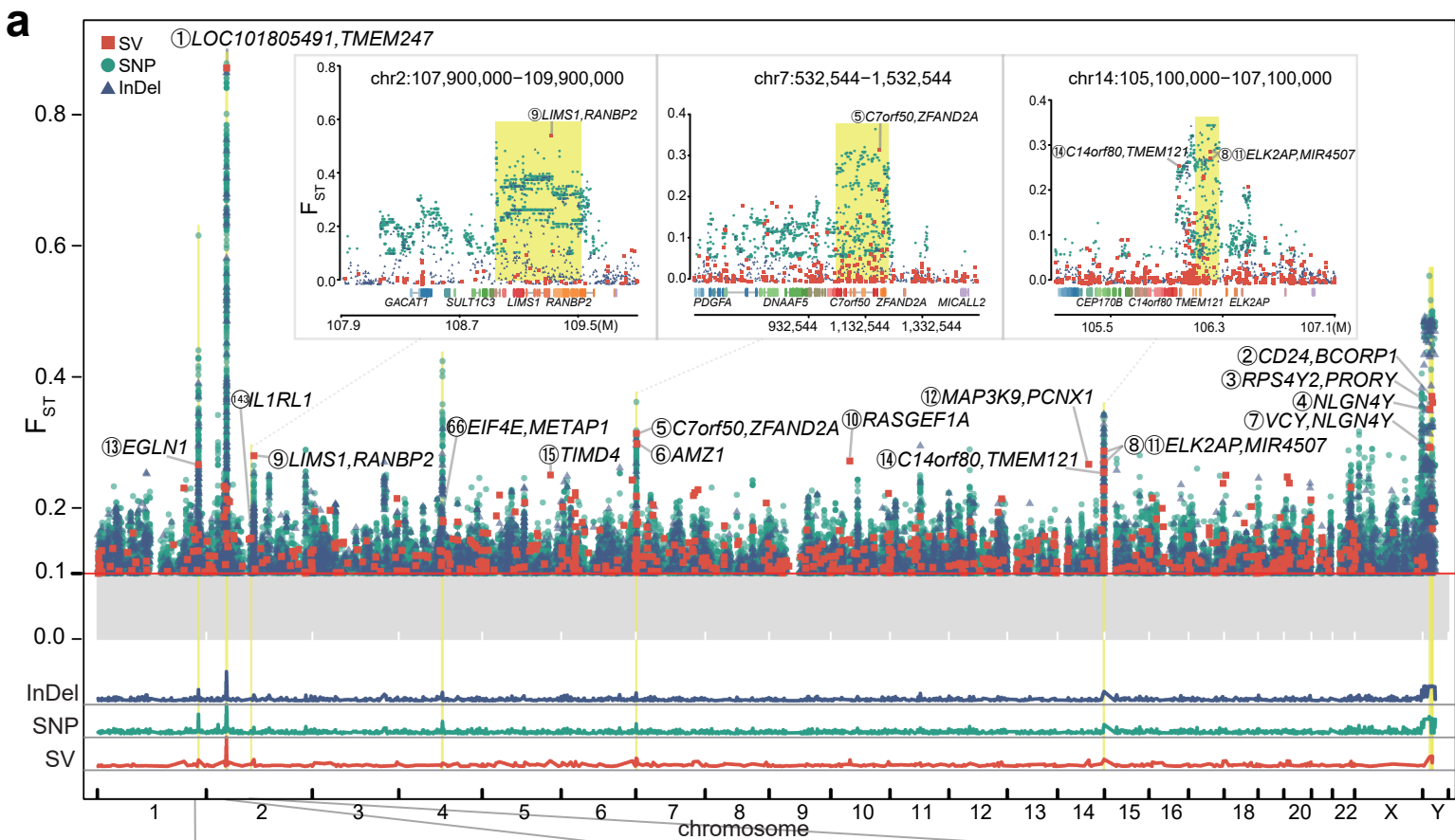


Figure 2. SV composition, length frequency, and chromosome distributions.



**Figure 3. Population genetics of Han-Tibetan populations.**

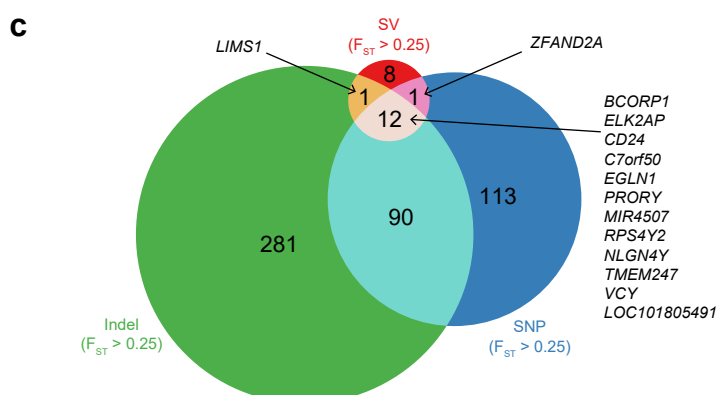
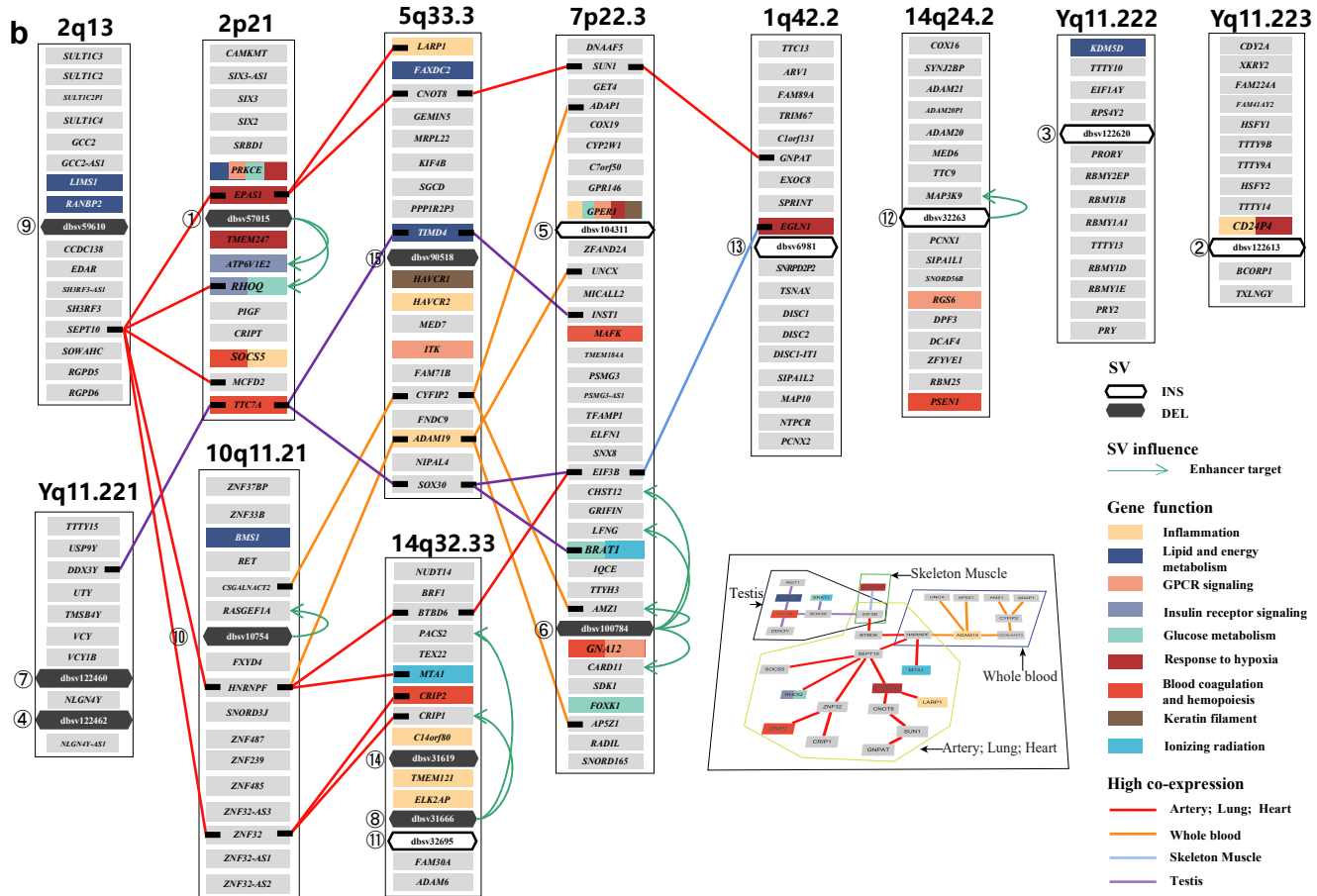


**Figure 4. Comparison of Han-Tibetan populations reveals the genetic landscape of evolutionary adaptation.**

Rank	Cytoband	Start Site	SV Length	$F_{ST}$	Tibetan Frequency	Han Frequency	SV Type	SV ID	Genomic Region	Gene
①	2p21	46,694,274	3408	0.87	0.93	0.04	Deletion	dbsv57015	Intergenic	<i>LOC101805491</i> ; <i>TMEM247</i>
②	Yq11.222	21,611,999	314	0.87	0.39	0.03	Insertion	dbsv122613	Intergenic	<i>CD24</i> <sup>#</sup> ; <i>BCORP1</i> <sup>#</sup>
③	Yq11.223	23,536,767	307	0.86	0.38	0.03	Insertion	dbsv122620	Intergenic	<i>RPS4Y</i> <sup>#</sup> ; <i>PRORY</i> <sup>#</sup>
④	Yq11.221	16,678,600	101	0.85	0.37	0.03	Deletion	dbsv122462*	Intronic	<i>NLGN4Y</i> <sup>#</sup>
⑤	7p22.3	1,186,212	160	0.31	0.32	0.75	Insertion	dbsv104311	Intergenic	<i>C7orf50</i> <sup>#</sup> ; <i>ZFAND2A</i> <sup>#</sup>
⑥	7p22.3	2,730,719	589	0.30	0.25	0.00	Deletion	dbsv100784	Intronic	<i>AMZ1</i> <sup>#</sup>
⑦	Yq11.221	16,533,228	76	0.29	0.45	0.09	Deletion	dbsv122460*	Intergenic	<i>VCY</i> <sup>#</sup> ; <i>NLGN4Y</i> <sup>#</sup>
⑧	14q32.33	106,211,066	158	0.29	0.08	0.46	Deletion	dbsv31666*	Intergenic	<i>ELK2AP</i> <sup>#</sup> ; <i>MIR4507</i> <sup>#</sup>
⑨	2q12.3	109,310,551	1557	0.28	0.27	0.01	Deletion	dbsv59610	Intergenic	<i>LIMS1</i> <sup>#</sup> ; <i>RANBP2</i> <sup>#</sup>
⑩	10q11.21	43,731,566	82	0.27	0.27	0.01	Deletion	dbsv10754	Intronic	<i>RASGEF1A</i> <sup>#</sup>
⑪	14q32.33	106,211,546	74	0.27	0.97	0.63	Insertion	dbsv32695*	Intergenic	<i>ELK2AP</i> <sup>#</sup> ; <i>MIR4507</i> <sup>#</sup>
⑫	14q24.2	71,280,282	125	0.27	0.32	0.04	Insertion	dbsv32263	Intergenic	<i>MAP3K9</i> <sup>#</sup> ; <i>PCNX1</i> <sup>#</sup>
⑬	1q42.2	231,526,826	131	0.27	0.30	0.78	Insertion	dbsv6981	Intronic	<i>EGLN1</i>
⑭	14q32.33	105,987,025	112	0.25	0.08	0.44	Deletion	dbsv31619*	Intergenic	<i>C14orf80</i> <sup>#</sup> ; <i>TMEM121</i> <sup>#</sup>
⑮	5q33.3	156,358,849	172	0.25	0.41	0.08	Deletion	dbsv90518*	Intronic	<i>TIMD4</i> <sup>#</sup>

\*Novel SV

#Novel high-altitude associated gene



**d** Relative Luciferase Activity

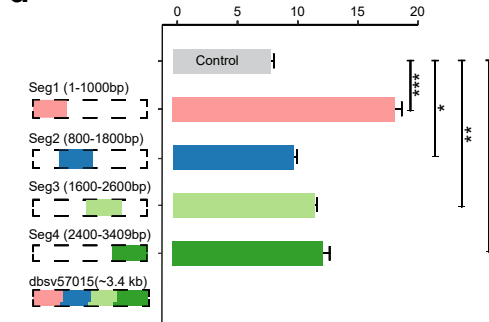


**Figure 5. Evolutionary selection of genes for adaptation to high altitude in Tibetans.**